Adv Comput Math (2022) 48:24
https://doi.org/10.1007/s10444-022-09948-0

Development and analysis of two new finite element schemes for a time-domain carpet cloak model

Jichun Li[1] · Chi-Wang Shu[2] · Wei Yang[3]

Received: 6 October 2021 / Accepted: 25 March 2022

Abstract

In this paper, we are concerned about a time-domain carpet cloak model, which was originally derived in our previous work Li et al. (*SIAM J. Appl. Math.*, *74*(4), pp. 1136–1151, 2014). Some finite element schemes have been developed for this model and used to simulate the cloaking phenomenon in Li et al. (*SIAM J. Appl. Math.*, *74*(4), pp. 1136–1151, 2014) and Li et al. (*Methods Appl. Math.*, *19*(2), pp. 359–378, 2019). However, numerical stabilities for those proposed explicit schemes are only proved under the time step constrain $\tau = O(h^2)$, which is impractical and too restricted. To overcome this disadvantage, we propose two new finite element schemes for solving this carpet cloak model: one is the implicit Crank-Nicolson (CN) scheme, and another one is the explicit leap-frog (LF) scheme. Inspired by a totally new energy developed for the continuous model, we prove the unconditional stability for the CN scheme and conditional stability for the LF scheme under the usual CFL constraint $\tau = O(h)$. Both numerical stabilities inherit the exact form as the continuous stability. Optimal error estimate is also established for the LF scheme. Finally, numerical results using the LF scheme are presented to support our analysis and demonstrate the cloaking phenomenon.

Communicated by: Ilaria Perugia

✉ Jichun Li
jichun.li@unlv.edu

Chi-Wang Shu
chi-wang_shu@brown.edu

Wei Yang
yangweixtu@126.com

[1] Department of Mathematical Sciences, University of Nevada, Las Vegas, NV 89154-4020, USA

[2] Division of Applied Mathematics, Brown University, Providence, RI, 02912, USA

[3] Hunan Key Laboratory for Computation and Simulation in Science Engineering, Xiangtan University, Xiangtan, China

Published online: 21 April 2022

Keywords Maxwell's equations · Finite element time-domain methods · Edge elements · Cloaking · Metamaterial

Mathematics Subject Classification (2010) 78M10 · 65N30 · 65F10 · 78-08

1 Introduction

Since the first successful construction of negative index metamaterial in 2000, the study of metamaterial has been a very hot research topic in sciences and engineering due to their many potential applications in subwavelength imaging, invisibility cloaks, and nano-optic devices, etc. Since Leonhardt and Pendry et al. [23, 41] independently proposed the idea of designing invisibility cloaks with metamaterials in 2006, there have been a growing interest in the study of cloaking devices. In addition to a great amount of publications in engineering and physics [27, 46], we have seen many excellent works published recently in mathematics community. For example, abstract mathematical analysis of cloaking phenomena has been done in [1, 14, 15, 20, 21], numerical analysis and simulations of cloaking phenomena have recently been carried out by the FDTD method [16, 19, 33], finite element method (FEM) [5, 22, 40], and the spectral element method [48, 49]. An interesting "carpet cloak" was proposed in 2008 by Li and Pendry [31] by using quasi-conformal mapping. Their strategy is to transform a bulging reflecting surface into a flat one, rendering anything within the bulging surface invisible from outside observers. Later on, experimental realizations of carpet cloaking were successfully demonstrated from microwave regime to terahertz and optical frequencies.

Broadband cloaking [15, 24, 34] inspires us to pursue the development and analysis of the finite element time-domain (FETD) method for cloaking simulation, which needs to solve the time-dependent Maxwell's equations in complex media [4, 25, 26, 44, 47]. Over the last three decades, many important results have been established for solving Maxwell's equations [3, 10, 11, 13]. For example, Monk [36] derived optimal approximation error estimates for edge element methods for the full time-dependent Maxwell system in homogeneous media. Ciarlet and Zou [8] were the first who derived the optimal approximation error estimates for edge element methods when the electric and magnetic fields are only regular in $H^{\alpha}(curl;\Omega)$ for $\frac{1}{2} < \alpha < 1$. More references can be found in some recent review papers [2, 7, 18] and related monographs [12, 17, 27, 37].

In 2014, Li and collaborators [29] carried out some preliminary mathematical analysis for the time-domain carpet cloak model. In [30], a revised FETD scheme was proposed and a corresponding stability was established. Unfortunately, the proofs of stabilities in [29, 30] were established with the impractical time step constraint $\tau = O(h^2)$. In this paper, we re-investigate this interesting carpet cloak model and find that a new energy is the key to reduce the time step constraint to $\tau = O(h)$, the usual requirement for those explicit FEM and FDTD schemes for solving time-dependent Maxwell's equations. With this newly discovered energy, we can establish a new continuous stability for the original cloak model. Then, we propose both an implicit Crank-Nicolson scheme and an explicit leap-frog scheme for solving the carpet cloak model. By following closely the proof of the continuous stability, we manage to prove the discrete stability for both schemes. Both schemes inherit beautifully the same stability established in the continuous case. Furthermore, the leap-frog scheme's stability is established under the usual time step constraint $\tau = O(h)$.

The rest of the paper is organized as follows. In Section 2, we present the carpet cloak model and establish a new stability which is different from our previous works [29, 30]. In Section 3, we propose a Crank-Nicolson scheme and prove its discrete stability which inherits the same form as the continuous case. Then, in Section 4, we propose a leap-frog scheme and carry out its stability analysis, which turns out just a minor change of the Crank-Nicolson scheme. We also present the optimal error estimate of the scheme. In Section 5, we present some numerical results to support our theoretical analysis. Finally, we conclude the paper in Section 6.

2 The carpet cloak model and its stability analysis

The governing equations for modeling the wave propagation in the carpet cloak are derived in [29] and given as follows (cf. [29, (2.3)-(2.5)]):

$$\partial_t \boldsymbol{D} = \nabla \times H, \tag{2.1}$$

$$\varepsilon_0 \lambda_2 \left(M_A^{-1} \partial_{t^2} \boldsymbol{E} + \omega_p^2 M_A^{-1} \boldsymbol{E} \right) = \partial_{t^2} \boldsymbol{D} + M_C \boldsymbol{D}, \tag{2.2}$$

$$\mu_0 \mu \partial_t H = -\nabla \times \boldsymbol{E}, \tag{2.3}$$

where we denote $\boldsymbol{D}$ for the 2D electric displacement, $\boldsymbol{E}$ for the 2D electric field, and H for the magnetic field. Furthermore, we denote $\partial_{t^k} u$ for the k-th derivative $\partial^k u / \partial t^k$ of a function u for any $k \geq 1$, we adopt the 2D vector and scalar curl operators:

$$\nabla \times H = (\frac{\partial H}{\partial y}, -\frac{\partial H}{\partial x})', \quad \nabla \times \boldsymbol{E} = \frac{\partial E_y}{\partial x} - \frac{\partial E_x}{\partial y}, \ \ \forall\, \boldsymbol{E} = (E_x, E_y)',$$

where E_x and E_y denote the x and y components of the electric field $\boldsymbol{E}$, respectively. Note that (2.2) is revised from [29, (2.4)] by left-multiplying both sides M_A^{-1} and denoting matrix $M_C = M_A^{-1} M_B$, where we denote M_A^{-1} as the inverse of matrix M_A, which is proved to be symmetric positive definite [29, Lemma 2.1]. The governing equations (2.1)–(2.3) hold true in the cloaking region formed by the cloaking region formed by the quadrilateral with vertices $(-d, 0)$, $(0, H_1)$, $(d, 0)$ and $(0, H_2)$, where d, H_1 and H_2 are positive constants and $H_2 > H_1 > 0$. The cloaked region, where the hiding objects can be placed, is formed by the triangle with vertices $(0, H_1)$, $(-d, 0)$ and $(d, 0)$.

In order to make those objects inside the cloaked region invisible, the permittivity and permeability in the cloaking region need to be specially designed and are given by [29]:

$$M_A = \begin{pmatrix} p_1^2 \lambda_2 + p_2^2 & p_2 p_4 + p_1 p_3 \lambda_2 \\ p_2 p_4 + p_1 p_3 \lambda_2 & p_3^2 \lambda_2 + p_4^2 \end{pmatrix}, \quad M_B = \begin{pmatrix} p_2^2 & p_2 p_4 \\ p_2 p_4 & p_4^2 \end{pmatrix} \omega_p^2, \tag{2.4}$$

where the positive constant ω_p is the plasma frequency resulting from the Drude dispersion model [29, p.1138], elements $p_i, i = 1, 2, 3, 4$, are

$$p_1=\sqrt{\frac{\lambda_2-a}{\lambda_2-\lambda_1}},\ \ p_2=-\sqrt{\frac{a-\lambda_1}{\lambda_2-\lambda_1}}\cdot \mathrm{sgn}(x),\ \ p_3=\sqrt{\frac{\lambda_2-c}{\lambda_2-\lambda_1}}\cdot \mathrm{sgn}(x),\ \ p_4=\sqrt{\frac{c-\lambda_1}{\lambda_2-\lambda_1}}, \tag{2.5}$$

and λ_1 and λ_2 are the eigenvalues of matrix ε given as:

$$\lambda_1=\frac{a+c-\sqrt{(a-c)^2+4b^2}}{2}, \quad \lambda_2=\frac{a+c+\sqrt{(a-c)^2+4b^2}}{2}. \tag{2.6}$$

To complete the carpet cloak model (2.1)–(2.3), we assume that (2.1)–(2.3) satisfy the initial conditions

$$\begin{aligned} &\boldsymbol{D}(\boldsymbol{x},0)=\boldsymbol{D}_0(\boldsymbol{x}), \quad \boldsymbol{E}(\boldsymbol{x},0)=\boldsymbol{E}_0(\boldsymbol{x}), \quad H(\boldsymbol{x},0)=H_0(\boldsymbol{x}),\\ &\partial_t\boldsymbol{D}(\boldsymbol{x},0)=\boldsymbol{D}_1(\boldsymbol{x}), \quad \partial_t\boldsymbol{E}(\boldsymbol{x},0)=\boldsymbol{E}_1(\boldsymbol{x}), \quad \forall\, \boldsymbol{x}\in\Omega, \end{aligned} \tag{2.7}$$

and the perfect conducting boundary condition (PEC):

$$\boldsymbol{n}\times\boldsymbol{E}=\boldsymbol{0} \quad \text{on } \partial\Omega, \tag{2.8}$$

where $\boldsymbol{D}_0$, $\boldsymbol{D}_1$, $\boldsymbol{E}_0$, $\boldsymbol{E}_1$ and H_0 are some properly given functions, $\boldsymbol{n}$ is the unit outward normal vector to $\partial\Omega$, and Ω denotes a polygonal domain in R^2.

Before we prove a novel stabilty for (2.1)–(2.3), we need to prove the following result.

Lemma 2.1 *The matrix $M_C := M_A^{-1}M_B$ is positive semi-definite.*

Proof Since M_A is symmetric positive definite [29, Lemma 2.1], its inverse M_A^{-1} exists and is given by

$$M_A^{-1}=\frac{1}{\det(M_A)}\begin{pmatrix} p_3^2\lambda_2+p_4^2 & -(p_2p_4+p_1p_3\lambda_2)\\ -(p_2p_4+p_1p_3\lambda_2) & p_1^2\lambda_2+p_2^2 \end{pmatrix}, \tag{2.9}$$

where $\det(M_A)$ is the determinant of M_A and is positive.

Through direct matrix multiplication, we have

$$M_A^{-1}M_B=\frac{\omega_p^2}{\det(M_A)}\cdot\lambda_2(p_1p_4-p_2p_3)\begin{pmatrix} -p_2p_3 & -p_3p_4\\ p_1p_2 & p_1p_4 \end{pmatrix}. \tag{2.10}$$

From (2.5) and (2.6), we easily obtain

$$p_1p_2=\sqrt{\frac{(\lambda_2-a)(a-\lambda_1)}{(\lambda_2-\lambda_1)^2}}\cdot\mathrm{sgn}(x)=\frac{\sqrt{\frac{\sqrt{(a-c)^2+4b^2}-(a-c)}{2}}\cdot\sqrt{\frac{\sqrt{(a-c)^2+4b^2}+(a-c)}{2}}}{\lambda_2-\lambda_1}\cdot\mathrm{sgn}(x),$$

$$-p_3p_4=\sqrt{\frac{(\lambda_2-c)(c-\lambda_1)}{(\lambda_2-\lambda_1)^2}}\cdot\mathrm{sgn}(x)=\frac{\sqrt{\frac{\sqrt{(a-c)^2+4b^2}+(a-c)}{2}}\cdot\sqrt{\frac{\sqrt{(a-c)^2+4b^2}-(a-c)}{2}}}{\lambda_2-\lambda_1}\cdot\mathrm{sgn}(x),$$

which shows that $p_1p_2 = -p_3p_4$. Hence, the matrix M_C is symmetric.

Furthermore, by (2.6), we see that

$$(\lambda_2-a)(c-\lambda_1) = \frac{c-a+\sqrt{(a-c)^2+4b^2}}{2}\cdot\frac{c-a+\sqrt{(a-c)^2+4b^2}}{2}, \quad (2.11)$$

$$(\lambda_2-c)(a-\lambda_1) = \frac{a-c+\sqrt{(a-c)^2+4b^2}}{2}\cdot\frac{a-c+\sqrt{(a-c)^2+4b^2}}{2}. \quad (2.12)$$

Hence, from (2.5), (2.6), and (2.11)–(2.12), we have

$$\begin{aligned} p_1p_4 - p_2p_3 &= \frac{\sqrt{(\lambda_2-a)(c-\lambda_1)}}{\lambda_2-\lambda_1} + \frac{\sqrt{(\lambda_2-c)(a-\lambda_1)}}{\lambda_2-\lambda_1} \\ &= \frac{(c-a)+\sqrt{(a-c)^2+4b^2}}{2(\lambda_2-\lambda_1)} + \frac{(a-c)+\sqrt{(a-c)^2+4b^2}}{2(\lambda_2-\lambda_1)} = \frac{\sqrt{(a-c)^2+4b^2}}{\lambda_2-\lambda_1} > 0. \quad (2.13)\end{aligned}$$

Finally, to prove that M_C is positive semi-definite, we want to find out its eigenvalues, which can be obtained by solving the following characteristic polynomial

$$\begin{aligned} 0 &= \begin{vmatrix} \xi + p_2p_3 & p_3p_4 \\ -p_1p_2 & \xi - p_1p_4 \end{vmatrix} = (\xi + p_2p_3)(\xi - p_1p_4) + p_1p_2p_3p_4 \\ &= \xi[\xi - (p_1p_4 - p_2p_3)], \quad (2.14)\end{aligned}$$

which yields $\xi_1 = 0$ and $\xi_2 = p_1p_4 - p_2p_3 > 0$ by (2.13), i.e., both eigenvalues of M_C are nonnegative. This shows that M_C is positive semi-definite. □

Since M_C is positive semi-definite, we can introduce its square root $M_C^{\frac{1}{2}}$. Below we establish a novel stability for (2.1)–(2.3), which is totally different from what we previously obtained in [29, 30] and provide an important guidance to the proof of discrete stability for the numerical scheme.

Theorem 2.2 *For the solution $(\boldsymbol{D}, H, \boldsymbol{E})$ of (2.1)–(2.3), denote the energy*

$$\begin{aligned} ENG(t) := \Big[&\varepsilon_0\lambda_2||M_A^{-\frac{1}{2}}\partial_{t^2}\boldsymbol{E}||^2 + 2\varepsilon_0\lambda_2\omega_p^2||M_A^{-\frac{1}{2}}\partial_t\boldsymbol{E}||^2 + \varepsilon_0\lambda_2\omega_p^4||M_A^{-\frac{1}{2}}\boldsymbol{E}||^2 \\ &+\frac{1}{\mu_0\mu}||\nabla\times\partial_t\boldsymbol{E}||^2 + \frac{\omega_p^2}{\mu_0\mu}||\nabla\times\boldsymbol{E}||^2 + ||\partial_t\boldsymbol{D}||^2 + ||M_C^{\frac{1}{2}}\boldsymbol{D}||^2\Big](t), \quad (2.15)\end{aligned}$$

where we denote $||\cdot||^2 := ||\cdot||^2_{L^2(\Omega)}$. Then, we have the following energy identity:

$$\begin{aligned} &ENG(t) - ENG(0) \\ &= 2\int_0^t \Big[\varepsilon_0\lambda_2(M_A^{-1}\partial_{t^2}\boldsymbol{E} + \omega_p^2 M_A^{-1}\boldsymbol{E}, \partial_t\boldsymbol{D}) + (M_C\partial_t\boldsymbol{D}, \partial_{t^2}\boldsymbol{E}) \\ &\quad +\omega_p^2(M_C\boldsymbol{D}, \partial_t\boldsymbol{E})\Big]dt. \quad (2.16)\end{aligned}$$

Furthermore, this leads to the stability:

$$ENG(t) \le ENG(0)\cdot\exp(C_*t), \quad \forall\, t \in [0, T], \quad (2.17)$$

where the constant $C_* > 0$ depends on the physical parameters $\varepsilon_0, \mu_0, d, H_1, H_2$ and ω_p.

Proof To make our proof easy to follow, we break it into several major steps.

(I). Multiplying (2.2) by $\partial_t \boldsymbol{D}$ and integrating the result over domain Ω, we have

$$\frac{1}{2}\frac{d}{dt}\left(||\partial_t \boldsymbol{D}||^2 + ||M_C^{\frac{1}{2}}\boldsymbol{D}||^2\right) = \varepsilon_0\lambda_2(M_A^{-1}\partial_{t^2}\boldsymbol{E} + \omega_p^2 M_A^{-1}\boldsymbol{E}, \partial_t \boldsymbol{D}). \quad (2.18)$$

Differentiating (2.2) with respect to t, we obtain

$$\varepsilon_0\lambda_2\left(M_A^{-1}\partial_{t^3}\boldsymbol{E} + \omega_p^2 M_A^{-1}\partial_t \boldsymbol{E}\right) = \partial_{t^3}\boldsymbol{D} + M_C\partial_t \boldsymbol{D}. \quad (2.19)$$

Multiplying (2.19) by $\partial_{t^2}\boldsymbol{E}$ and integrating the result over domain Ω, we have

$$\frac{\varepsilon_0\lambda_2}{2}\frac{d}{dt}\left(||M_A^{-\frac{1}{2}}\partial_{t^2}\boldsymbol{E}||^2 + \omega_p^2||M_A^{-\frac{1}{2}}\partial_t \boldsymbol{E}||^2\right) = (\partial_{t^3}\boldsymbol{D} + M_C\partial_t \boldsymbol{D}, \partial_{t^2}\boldsymbol{E}). \quad (2.20)$$

(II). Differentiating (2.1) with respect to t twice, and using the differentiation of (2.3) with respect to t once, we obtain

$$\partial_{t^3}\boldsymbol{D} = \nabla\times\partial_{t^2}\boldsymbol{H} = \frac{-1}{\mu_0\mu}\nabla\times\nabla\times\partial_t \boldsymbol{E}. \quad (2.21)$$

Now, multiplying (2.21) by $\partial_{t^2}\boldsymbol{E}$, integrating over domain Ω, and using integration by parts and the PEC boundary condition (2.8), we have

$$\begin{aligned}(\partial_{t^3}\boldsymbol{D}, \partial_{t^2}\boldsymbol{E}) &= \frac{-1}{\mu_0\mu}(\nabla\times\nabla\times\partial_t \boldsymbol{E}, \partial_{t^2}\boldsymbol{E})\\ &= \frac{-1}{\mu_0\mu}(\nabla\times\partial_t \boldsymbol{E}, \nabla\times\partial_{t^2}\boldsymbol{E}) = \frac{-1}{2\mu_0\mu}\frac{d}{dt}||\nabla\times\partial_t \boldsymbol{E}||^2. \quad (2.22)\end{aligned}$$

Adding (2.18), (2.20) and (2.22) together, we obtain

$$\begin{aligned}&\frac{1}{2}\frac{d}{dt}\Big(||\partial_t \boldsymbol{D}||^2 + ||M_C^{\frac{1}{2}}\boldsymbol{D}||^2 + \varepsilon_0\lambda_2(||M_A^{-\frac{1}{2}}\partial_{t^2}\boldsymbol{E}||^2 + \omega_p^2||M_A^{-\frac{1}{2}}\partial_t \boldsymbol{E}||^2)\\ &+\frac{1}{\mu_0\mu}||\nabla\times\partial_t \boldsymbol{E}||^2\Big)\\ &= \varepsilon_0\lambda_2(M_A^{-1}\partial_{t^2}\boldsymbol{E} + \omega_p^2 M_A^{-1}\boldsymbol{E}, \partial_t \boldsymbol{D}) + (M_C\partial_t \boldsymbol{D}, \partial_{t^2}\boldsymbol{E}). \quad (2.23)\end{aligned}$$

(III). Note that all right-hand side (RHS) terms of (2.23) can be controlled by the corresponding left-hand side (LHS) terms except that $\boldsymbol{E}$ term in $(M_A^{-1}\boldsymbol{E}, \partial_t \boldsymbol{D})$. To control this, we multiply (2.2) by $\partial_t \boldsymbol{E}$ and integrate over domain Ω to obtain

$$\frac{\varepsilon_0\lambda_2}{2}\frac{d}{dt}\left(||M_A^{-\frac{1}{2}}\partial_t \boldsymbol{E}||^2 + \omega_p^2||M_A^{-\frac{1}{2}}\boldsymbol{E}||^2\right) = (\partial_{t^2}\boldsymbol{D} + M_C\boldsymbol{D}, \partial_t \boldsymbol{E}). \quad (2.24)$$

To bound the $\partial_{t^2}\boldsymbol{D}$ term in (2.24), using (2.1), (2.3), and integration by parts, we have

$$\begin{aligned}(\partial_{t^2}\boldsymbol{D}, \partial_t \boldsymbol{E}) &= (\nabla\times\partial_t H, \partial_t \boldsymbol{E}) = \frac{-1}{\mu_0\mu}(\nabla\times\nabla\times\boldsymbol{E}, \partial_t \boldsymbol{E})\\ &= \frac{-1}{\mu_0\mu}(\nabla\times\boldsymbol{E}, \nabla\times\partial_t \boldsymbol{E}) = \frac{-1}{2\mu_0\mu}\frac{d}{dt}||\nabla\times\boldsymbol{E}||^2. \quad (2.25)\end{aligned}$$

Substituting (2.25) into (2.24), multiplying the result by ω_p^2, then adding the result to (2.23), we have

$$\begin{aligned}\frac{1}{2}\frac{d}{dt}ENG(t) &= \varepsilon_0\lambda_2(M_A^{-}\partial_{t^2}\boldsymbol{E} + \omega_p^2 M_A^{-1}\boldsymbol{E}, \partial_t \boldsymbol{D}) \\ &\quad + (M_C\partial_t\boldsymbol{D}, \partial_{t^2}\boldsymbol{E}) + \omega_p^2(M_C\boldsymbol{D}, \partial_t\boldsymbol{E}). \end{aligned} \tag{2.26}$$

Integrating (2.26) with respect to t from 0 to t, we obtain the energy identity (2.16). Then, applying the Cauchy-Schwarz inequality to all RHS terms of (2.16) and the Gronwall inequality, we complete the proof. □

3 The Crank-Nicolson scheme and its stability analysis

To solve our carpet model, we assume that domain Ω is partitioned by a family of regular rectangular or triangular mesh T^h with maximum mesh size h, and adopt the standard Raviart-Thomas-Nédélec (RTN) mixed finite element spaces U_h and $\boldsymbol{V}_h$ (cf. [6, 38, 39, 43]): For rectangular elements $K \in T^h$ and any integer $p \geq 0$,

$$\begin{aligned} U_h &= \{\psi_h \in L^2(\Omega): \ \ \psi_h|_K \in Q_{p,p}, \ \forall\, K \in T^h\}, \\ \boldsymbol{V}_h &= \{\boldsymbol{\phi}_h \in H(curl;\Omega): \ \ \boldsymbol{\phi}_h|_K \in Q_{p,p+1}\times Q_{p+1,p}, \ \forall\, K \in T^h\}, \end{aligned} \tag{3.1}$$

where $Q_{i,j}$ denotes the space of polynomials whose degrees are less than or equal to i and j in variables x and y, respectively. For triangular elements, the RTN spaces can be defined also. To accommodate the PEC boundary condition (2.8), we introduce the subspace

$$\boldsymbol{V}_h^0 = \{\boldsymbol{\phi}_h \in \boldsymbol{V}_h: \ \ \boldsymbol{n}\times\boldsymbol{\phi}_h = \boldsymbol{0} \ \text{ on } \partial\Omega\}.$$

To carry out a time discretization, we divide the time interval $I = [0, T]$ into N uniform subintervals $I_i = [t_{i-1}, t_i]$ by points $t_n = n\tau$, $n = 0, 1, ..., N$, where $\tau = \frac{T}{N}$. Furthermore, we introduce the following standard averaging operators: For any time sequence function u^n,

$$\overline{u}^{n+\frac{1}{2}} := \frac{u^{n+1}+u^n}{2}, \quad \widetilde{u}^n := \frac{u^{n+1}+u^{n-1}}{2},$$

and central difference operators in time:

$$\delta_\tau u^{n+\frac{1}{2}} := \frac{u^{n+1}-u^n}{\tau}, \quad \delta_\tau^2 u^n := \frac{\delta_\tau u^{n+\frac{1}{2}} - \delta_\tau u^{n-\frac{1}{2}}}{\tau} = \frac{u^{n+1}-2u^n+u^{n-1}}{\tau^2}.$$

First, let us construct the following Crank-Nicolson (CN) scheme for solving the model (2.1)-(2.3): For $n \geq 0$ find $\boldsymbol{D}_h^{n+1}, \boldsymbol{E}_h^{n+1} \in \boldsymbol{V}_h^0$, $H_h^{n+1} \in U_h$ such that

$$\left(\delta_\tau \boldsymbol{D}_h^{n+\frac{1}{2}}, \boldsymbol{\phi}_h\right) = (\overline{H}_h^{n+\frac{1}{2}}, \nabla\times\boldsymbol{\phi}_h), \tag{3.2}$$

$$\varepsilon_0\lambda_2\left(M_A^{-1}\delta_\tau^2\boldsymbol{E}_h^n + \omega_p^2 M_A^{-1}\widetilde{\boldsymbol{E}}_h^n, \boldsymbol{\phi}_h\right) = \left(\delta_\tau^2\boldsymbol{D}_h^n + M_C\widetilde{\boldsymbol{D}}_h^n, \boldsymbol{\phi}_h\right), \tag{3.3}$$

$$\mu_0\mu\left(\delta_\tau H_h^{n+\frac{1}{2}}, \psi_h\right) = -(\nabla\times\overline{\boldsymbol{E}}_h^{n+\frac{1}{2}}, \psi_h), \tag{3.4}$$

hold true for any $\boldsymbol{\phi}_h \in \boldsymbol{V}_h^0$ and $\psi_h \in U_h$. The needed initial approximations $H_h^0, \boldsymbol{D}_h^0, \boldsymbol{E}_h^0, \boldsymbol{D}_h^{-1}, \boldsymbol{E}_h^{-1}$ can be obtained from discretizing the given initial conditions (2.7) as follows:

$$\begin{aligned} &\boldsymbol{D}_h^0 = \Pi_c \boldsymbol{D}_0, \quad \boldsymbol{E}_h^0 = \Pi_c \boldsymbol{E}_0, \quad H_h^0 = \Pi_2 H_0, \\ &\delta_{2\tau}\boldsymbol{D}_h^0 := \frac{\boldsymbol{D}_h^1 - \boldsymbol{D}_h^{-1}}{2\tau} = \Pi_c \boldsymbol{D}_1, \quad \delta_{2\tau}\boldsymbol{E}_h^0 := \frac{\boldsymbol{E}_h^1 - \boldsymbol{E}_h^{-1}}{2\tau} = \Pi_c \boldsymbol{E}_1, \end{aligned} \tag{3.5}$$

where Π_c and Π_2 are the Nédélec interpolation and L^2 projection operators in space $\boldsymbol{V}_h$ and into space U_h, respectively. It is known that the following interpolation and projection error estimates hold true (cf. [27, 37]):

$$||\boldsymbol{u} - \Pi_c \boldsymbol{u}||_{H(\text{curl};\Omega)} \leq ch^p ||\boldsymbol{u}||_{H^p(\text{curl};\Omega)}, \quad \forall\, \boldsymbol{u} \in H^p(\text{curl};\, \Omega), \tag{3.6}$$

$$||u - \Pi_2 u||_{L^2(\Omega)} \leq ch^p ||u||_{H^p(\Omega)}, \quad \forall\, u \in H^p(\Omega), \tag{3.7}$$

where we denote the norm $||u||_{H^p(\Omega)}$ for the Sobolev space $H^p(\Omega)$, and norm $||\boldsymbol{u}||_{H^s(\text{curl};\Omega)} := (||\boldsymbol{u}||^2_{(H^s(\Omega))^2} + ||\nabla \times \boldsymbol{u}||^2_{H^s(\Omega)})^{1/2}$ for the Sobolev space

$$H^s(\text{curl};\, \Omega) = \{\boldsymbol{u} \in (H^s(\Omega))^2 \mid \nabla \times \boldsymbol{u} \in H^s(\Omega)\}.$$

In the rest of this section, we will show that the scheme (3.2)–(3.4) satisfies a discrete stability, which is the discrete form of the continuous stability proved in Theorem 2.1.

To prove a discrete stability, we will use the following discrete Gronwall inequality.

Lemma 3.1 [42, Lemma 1.4.2] *Assume that the sequence u_n satisfies*

$$u_0 \leq g_0, \quad \textit{and} \quad u_n \leq g_0 + r\tau \sum_{s=0}^{n-1} u_s, \ \forall\, n \geq 1,$$

for some positive constants g_0, r and τ. Then, u_n satisfies

$$u_n \leq g_0 \cdot (1 + r\tau)^n \leq g_0 \cdot \exp(rn\tau), \quad \forall\, n \geq 1.$$

Let us introduce the induced matrix norm. For a $s \times s$ matrix A, we denote

$$||A||_2 = \sup_{0 \neq u \in R^s} \frac{||Au||_2}{||u||_2}.$$

Now, we present the proof of an unconditional stability for our proposed CN scheme (3.2)–(3.4) given in Theorem 3.1.

Theorem 3.2 *For the FE solution $(\boldsymbol{D}_h^{n+1}, \boldsymbol{E}_h^{n+1}, H_h^{n+1})$ of the CN scheme (3.2)–(3.4), denote the discrete energy at time level n:*

$$\begin{aligned} ENG_{cn}(n) &:= ||\delta_\tau \boldsymbol{D}_h^{n+\frac{1}{2}}||^2 + \frac{||M_C^{\frac{1}{2}} \boldsymbol{D}_h^{n+1}||^2 + ||M_C^{\frac{1}{2}} \boldsymbol{D}_h^n||^2}{2} + \varepsilon_0 \lambda_2 ||M_A^{-\frac{1}{2}} \delta_\tau^2 \boldsymbol{E}_h^n||^2 \\ &+ \varepsilon_0 \lambda_2 \omega_p^2 \left[\frac{||M_A^{-\frac{1}{2}} \delta_\tau \boldsymbol{E}_h^{n+\frac{1}{2}}||^2 + ||M_A^{-\frac{1}{2}} \delta_\tau \boldsymbol{E}_h^{n-\frac{1}{2}}||^2}{2} + ||M_A^{-\frac{1}{2}} \delta_\tau \boldsymbol{E}_h^{n+\frac{1}{2}}||^2 \right] \end{aligned} \tag{3.8}$$

$$+\frac{1}{\mu_0\mu}||\nabla\times\delta_\tau\overline{\boldsymbol{E}}_h^n||^2+\varepsilon_0\lambda_2\omega_p^4\left(\frac{||M_A^{-\frac{1}{2}}\boldsymbol{E}_h^{n+1}||^2+||M_A^{-\frac{1}{2}}\boldsymbol{E}_h^n||^2}{2}\right)$$
$$+\frac{\omega_p^2}{\mu_0\mu}||\nabla\times\overline{\boldsymbol{E}}_h^{n+\frac{1}{2}}||^2.$$

Suppose that the time step size satisfies the constraint

$$\tau\leq\min\left\{1/\left(\sqrt{\varepsilon_0\lambda_2}||M_A^{-\frac{1}{2}}||_2+\frac{||M_A^{-\frac{1}{2}}M_B||_2}{2\sqrt{\varepsilon_0\lambda_2}}\right),\frac{\sqrt{\varepsilon_0\lambda_2}}{\omega_p||M_C^{\frac{1}{2}}M_A^{\frac{1}{2}}||_2}\right\},\tag{3.9}$$

then we have

$$ENG_{cn}(m)\leq 2ENG_{cn}(0)\cdot\exp(2m\tau),\quad\forall\, m\geq 1.$$

Remark 3.3 We like to remark that the time step constraint (3.9) only depends on those model physical parameters, but is independent of mesh size h. Hence, the CN scheme (3.2)-(3.4) is unconditionally stable.

Proof The proof follows closely to the continuous case given for Theorem 2.1, and is also composed of several major parts.

(I). Choosing $\boldsymbol{\phi}_h=\tau\delta_\tau\overline{\boldsymbol{D}}_h^n$ in (3.3), and using the following identities:

$$(\delta_\tau^2\boldsymbol{D}_h^n,\tau\delta_\tau\overline{\boldsymbol{D}}_h^n)=(\frac{\delta_\tau\boldsymbol{D}_h^{n+\frac{1}{2}}-\delta_\tau\boldsymbol{D}_h^{n-\frac{1}{2}}}{\tau},\tau\cdot\frac{\delta_\tau\boldsymbol{D}_h^{n+\frac{1}{2}}+\delta_\tau\boldsymbol{D}_h^{n-\frac{1}{2}}}{2})$$
$$=\frac{1}{2}(||\delta_\tau\boldsymbol{D}_h^{n+\frac{1}{2}}||^2-||\delta_\tau\boldsymbol{D}_h^{n-\frac{1}{2}}||^2),\tag{3.10}$$

and

$$\begin{aligned}(M_C\widetilde{\boldsymbol{D}}_h^n,\tau\delta_\tau\overline{\boldsymbol{D}}_h^n)&=(M_C\frac{\boldsymbol{D}_h^{n+1}+\boldsymbol{D}_h^{n-1}}{2},\tau\cdot\frac{\delta_\tau\boldsymbol{D}_h^{n+\frac{1}{2}}+\delta_\tau\boldsymbol{D}_h^{n-\frac{1}{2}}}{2})\\&=(M_C\frac{\boldsymbol{D}_h^{n+1}+\boldsymbol{D}_h^{n-1}}{2},\frac{(\boldsymbol{D}_h^{n+1}-\boldsymbol{D}_h^n)+(\boldsymbol{D}_h^n-\boldsymbol{D}_h^{n-1})}{2})\\&=\frac{1}{4}(||M_C^{\frac{1}{2}}\boldsymbol{D}_h^{n+1}||^2-||M_C^{\frac{1}{2}}\boldsymbol{D}_h^{n-1}||^2),\end{aligned}\tag{3.11}$$

we have

$$\frac{1}{2}(||\delta_\tau\boldsymbol{D}_h^{n+\frac{1}{2}}||^2-||\delta_\tau\boldsymbol{D}_h^{n-\frac{1}{2}}||^2)+\frac{1}{4}(||M_C^{\frac{1}{2}}\boldsymbol{D}_h^{n+1}||^2-||M_C^{\frac{1}{2}}\boldsymbol{D}_h^{n-1}||^2)$$
$$=\tau\varepsilon_0\lambda_2\left(M_A^{-1}\delta_\tau^2\boldsymbol{E}_h^n+\omega_p^2M_A^{-1}\widetilde{\boldsymbol{E}}_h^n,\delta_\tau\overline{\boldsymbol{D}}_h^n\right).\tag{3.12}$$

(II). Using (3.3) with n increased to $n+1$ to subtract (3.3), then dividing the result by τ, we obtain

$$\varepsilon_0\lambda_2\left(M_A^{-1}\frac{\delta_\tau^2\boldsymbol{E}_h^{n+1}-\delta_\tau^2\boldsymbol{E}_h^n}{\tau}+\omega_p^2M_A^{-1}\frac{\widetilde{\boldsymbol{E}}_h^{n+1}-\widetilde{\boldsymbol{E}}_h^n}{\tau},\boldsymbol{\phi}_h\right)$$
$$=\left(\frac{\delta_\tau^2\boldsymbol{D}_h^{n+1}-\delta_\tau^2\boldsymbol{D}_h^n}{\tau}+M_C\frac{\widetilde{\boldsymbol{D}}_h^{n+1}-\widetilde{\boldsymbol{D}}_h^n}{\tau},\boldsymbol{\phi}_h\right). \tag{3.13}$$

Using (3.2) and (3.4), we have

$$\left(\frac{\delta_\tau^2\boldsymbol{D}_h^{n+1}-\delta_\tau^2\boldsymbol{D}_h^n}{\tau},\boldsymbol{\phi}_h\right)=\left(\frac{(\delta_\tau\boldsymbol{D}_h^{n+\frac{3}{2}}-\delta_\tau\boldsymbol{D}_h^{n+\frac{1}{2}})-(\delta_\tau\boldsymbol{D}_h^{n+\frac{1}{2}}-\delta_\tau\boldsymbol{D}_h^{n-\frac{1}{2}})}{\tau^2},\boldsymbol{\phi}_h\right)$$
$$\overset{by(3.2)}{=}\left(\frac{(\overline{H}_h^{n+\frac{3}{2}}-\overline{H}_h^{n+\frac{1}{2}})-(\overline{H}_h^{n+\frac{1}{2}}-\overline{H}_h^{n-\frac{1}{2}})}{\tau^2},\nabla\times\boldsymbol{\phi}_h\right)$$
$$=\left(\frac{\delta_\tau\overline{H}_h^{n+1}-\delta_\tau\overline{H}_h^n}{\tau},\nabla\times\boldsymbol{\phi}_h\right)$$
$$=\left(\frac{(\delta_\tau H_h^{n+\frac{3}{2}}+\delta_\tau H_h^{n+\frac{1}{2}})-(\delta_\tau H_h^{n+\frac{1}{2}}+\delta_\tau H_h^{n-\frac{1}{2}})}{2\tau},\nabla\times\boldsymbol{\phi}_h\right)$$
$$=\left(\frac{(\delta_\tau H_h^{n+\frac{3}{2}}-\delta_\tau H_h^{n+\frac{1}{2}})+(\delta_\tau H_h^{n+\frac{1}{2}}-\delta_\tau H_h^{n-\frac{1}{2}})}{2\tau},\nabla\times\boldsymbol{\phi}_h\right)$$
$$\overset{by(3.4)}{=}\frac{-1}{2\mu_0\mu}\left(\nabla\times\frac{\overline{\boldsymbol{E}}_h^{n+\frac{3}{2}}-\overline{\boldsymbol{E}}_h^{n+\frac{1}{2}}}{\tau}+\nabla\times\frac{\overline{\boldsymbol{E}}_h^{n+\frac{1}{2}}-\overline{\boldsymbol{E}}_h^{n-\frac{1}{2}}}{\tau},\nabla\times\boldsymbol{\phi}_h\right)$$
$$=\frac{-1}{2\mu_0\mu}\left(\nabla\times\delta_\tau\overline{\boldsymbol{E}}_h^{n+1}+\nabla\times\delta_\tau\overline{\boldsymbol{E}}_h^n,\nabla\times\boldsymbol{\phi}_h\right), \tag{3.14}$$

where in the above derivation, we used the fact that $\nabla\times\boldsymbol{\phi}_h\in U_h$ for any $\boldsymbol{\phi}_h\in\boldsymbol{V}_h$.

Choosing $\boldsymbol{\phi}_h=\tau\delta_\tau^2\overline{\boldsymbol{E}}_h^{n+\frac{1}{2}}=\frac{\tau}{2}(\delta_\tau^2\boldsymbol{E}_h^{n+1}+\delta_\tau^2\boldsymbol{E}_h^n)$ in (3.13), then using the fact that $\boldsymbol{\phi}_h=\delta_\tau\overline{\boldsymbol{E}}_h^{n+1}-\delta_\tau\overline{\boldsymbol{E}}_h^n$ in (3.14), we have

$$\frac{\varepsilon_0\lambda_2}{2}(||M_A^{-\frac{1}{2}}\delta_\tau^2\boldsymbol{E}_h^{n+1}||^2-||M_A^{-\frac{1}{2}}\delta_\tau^2\boldsymbol{E}_h^n||^2)$$
$$+\frac{\varepsilon_0\lambda_2\omega_p^2}{4}(||M_A^{-\frac{1}{2}}\delta_\tau\boldsymbol{E}_h^{n+\frac{3}{2}}||^2-||M_A^{-\frac{1}{2}}\delta_\tau\boldsymbol{E}_h^{n-\frac{1}{2}}||^2)$$
$$+\frac{1}{2\mu_0\mu}(||\nabla\times\delta_\tau\overline{\boldsymbol{E}}_h^{n+1}||^2-||\nabla\times\delta_\tau\overline{\boldsymbol{E}}_h^n||^2)=\tau(M_C\delta_\tau\widetilde{\boldsymbol{D}}_h^{n+\frac{1}{2}},\delta_\tau^2\overline{\boldsymbol{E}}_h^{n+\frac{1}{2}}), \tag{3.15}$$

where we used the following facts

$$\frac{\widetilde{\boldsymbol{E}}_h^{n+1}-\widetilde{\boldsymbol{E}}_h^{n}}{\tau}=\frac{(\boldsymbol{E}_h^{n+2}+\boldsymbol{E}_h^{n})-(\boldsymbol{E}_h^{n+1}+\boldsymbol{E}_h^{n-1})}{2\tau}$$
$$=\frac{(\boldsymbol{E}_h^{n+2}-\boldsymbol{E}_h^{n+1})+(\boldsymbol{E}_h^{n}-\boldsymbol{E}_h^{n-1})}{2\tau}=\frac{1}{2}(\delta_\tau\boldsymbol{E}_h^{n+\frac{3}{2}}+\delta_\tau\boldsymbol{E}_h^{n-\frac{1}{2}}), \quad (3.16)$$

and

$$\boldsymbol{\phi}_h=\delta_\tau\overline{\boldsymbol{E}}_h^{n+1}-\delta_\tau\overline{\boldsymbol{E}}_h^{n}=\delta_\tau\left(\frac{\boldsymbol{E}_h^{n+\frac{3}{2}}+\boldsymbol{E}_h^{n+\frac{1}{2}}}{2}-\frac{\boldsymbol{E}_h^{n+\frac{1}{2}}+\boldsymbol{E}_h^{n-\frac{1}{2}}}{2}\right)$$
$$=\delta_\tau\left(\frac{\boldsymbol{E}_h^{n+\frac{3}{2}}-\boldsymbol{E}_h^{n-\frac{1}{2}}}{2}\right). \quad (3.17)$$

(III). Choosing $\boldsymbol{\phi}_h=\tau\delta_\tau\overline{\boldsymbol{E}}_h^{n}$ in (3.3), and by the same argument as (I), we have

$$\frac{\varepsilon_0\lambda_2}{2}(||M_A^{-\frac{1}{2}}\delta_\tau\boldsymbol{E}_h^{n+\frac{1}{2}}||^2-||M_A^{-\frac{1}{2}}\delta_\tau\boldsymbol{E}_h^{n-\frac{1}{2}}||^2)$$
$$+\frac{\varepsilon_0\lambda_2\omega_p^2}{4}(||M_A^{-\frac{1}{2}}\boldsymbol{E}_h^{n+1}||^2-||M_A^{-\frac{1}{2}}\boldsymbol{E}_h^{n-1}||^2)$$
$$=\tau\left(\delta_\tau^2\boldsymbol{D}_h^n+M_C\widetilde{\boldsymbol{D}}_h^n,\delta_\tau\overline{\boldsymbol{E}}_h^n\right). \quad (3.18)$$

To control the term $\delta_\tau^2\boldsymbol{D}_h^n$ on the RHS of (3.18), by using (3.2) and (3.4), we see that

$$\tau(\delta_\tau^2\boldsymbol{D}_h^n,\delta_\tau\overline{\boldsymbol{E}}_h^n)=(\delta_\tau\boldsymbol{D}_h^{n+\frac{1}{2}}-\delta_\tau\boldsymbol{D}_h^{n-\frac{1}{2}},\delta_\tau\overline{\boldsymbol{E}}_h^n)$$
$$\overset{by(3.2)}{=}(\overline{H}_h^{n+\frac{1}{2}}-\overline{H}_h^{n-\frac{1}{2}},\nabla\times\delta_\tau\overline{\boldsymbol{E}}_h^n)=\tau(\delta_\tau\overline{H}_h^n,\nabla\times\delta_\tau\overline{\boldsymbol{E}}_h^n)$$
$$=\frac{\tau}{2}(\delta_\tau H_h^{n+\frac{1}{2}}+\delta_\tau H_h^{n-\frac{1}{2}},\nabla\times\delta_\tau\overline{\boldsymbol{E}}_h^n)$$
$$\overset{by(3.4)}{=}\frac{-\tau}{2\mu_0\mu}(\nabla\times\overline{\boldsymbol{E}}_h^{n+\frac{1}{2}}+\nabla\times\overline{\boldsymbol{E}}_h^{n-\frac{1}{2}},\nabla\times\delta_\tau\overline{\boldsymbol{E}}_h^n)$$
$$=\frac{-1}{2\mu_0\mu}(\nabla\times\overline{\boldsymbol{E}}_h^{n+\frac{1}{2}}+\nabla\times\overline{\boldsymbol{E}}_h^{n-\frac{1}{2}},\nabla\times\overline{\boldsymbol{E}}_h^{n+\frac{1}{2}}-\nabla\times\overline{\boldsymbol{E}}_h^{n-\frac{1}{2}})$$
$$=\frac{-1}{2\mu_0\mu}\left(||\nabla\times\overline{\boldsymbol{E}}_h^{n+\frac{1}{2}}||^2-||\nabla\times\overline{\boldsymbol{E}}_h^{n-\frac{1}{2}}||^2\right). \quad (3.19)$$

(IV). Note that term $\delta_\tau\widetilde{\boldsymbol{D}}_h^{n+\frac{1}{2}}=\frac{\delta_\tau\boldsymbol{D}_h^{n+\frac{3}{2}}+\delta_\tau\boldsymbol{D}_h^{n-\frac{1}{2}}}{2}$ in (3.15) can not be controlled by the like term on the LHS of (3.12). Hence, we add (3.15) with all n's reduced by one to (3.12), and (3.18) multiplied by ω_p^2 with the substitution of (3.19), we obtain

$$\frac{1}{2}(||\delta_\tau\boldsymbol{D}_h^{n+\frac{1}{2}}||^2-||\delta_\tau\boldsymbol{D}_h^{n-\frac{1}{2}}||^2)+\frac{1}{4}(||M_C^{\frac{1}{2}}\boldsymbol{D}_h^{n+1}||^2-||M_C^{\frac{1}{2}}\boldsymbol{D}_h^{n-1}||^2)$$
$$+\frac{\varepsilon_0\lambda_2}{2}(||M_A^{-\frac{1}{2}}\delta_\tau^2\boldsymbol{E}_h^n||^2-||M_A^{-\frac{1}{2}}\delta_\tau^2\boldsymbol{E}_h^{n-1}||^2)$$

$$
\begin{aligned}
&+\frac{\varepsilon_0\lambda_2\omega_p^2}{4}(||M_A^{-\frac{1}{2}}\delta_\tau \boldsymbol{E}_h^{n+\frac{1}{2}}||^2-||M_A^{-\frac{1}{2}}\delta_\tau \boldsymbol{E}_h^{n-\frac{3}{2}}||^2)\\
&+\frac{1}{2\mu_0\mu}(||\nabla\times\delta_\tau\overline{\boldsymbol{E}}_h^n||^2-||\nabla\times\delta_\tau\overline{\boldsymbol{E}}_h^{n-1}||^2)\\
&+\frac{\varepsilon_0\lambda_2\omega_p^2}{2}(||M_A^{-\frac{1}{2}}\delta_\tau \boldsymbol{E}_h^{n+\frac{1}{2}}||^2-||M_A^{-\frac{1}{2}}\delta_\tau \boldsymbol{E}_h^{n-\frac{1}{2}}||^2)\\
&+\frac{\varepsilon_0\lambda_2\omega_p^4}{4}(||M_A^{-\frac{1}{2}}\boldsymbol{E}_h^{n+1}||^2-||M_A^{-\frac{1}{2}}\boldsymbol{E}_h^{n-1}||^2)\\
&+\frac{\omega_p^2}{2\mu_0\mu}\left(||\nabla\times\overline{\boldsymbol{E}}_h^{n+\frac{1}{2}}||^2-||\nabla\times\overline{\boldsymbol{E}}_h^{n-\frac{1}{2}}||^2\right)\\
=\ &\tau\varepsilon_0\lambda_2\left(M_A^{-1}\delta_\tau^2\boldsymbol{E}_h^n+\omega_p^2M_A^{-1}\widetilde{\boldsymbol{E}}_h^n,\delta_\tau\overline{\boldsymbol{D}}_h^n\right)\\
&\quad+\tau(M_C\delta_\tau\widetilde{\boldsymbol{D}}_h^{n-\frac{1}{2}},\delta_\tau^2\overline{\boldsymbol{E}}_h^{n-\frac{1}{2}})+\tau\omega_p^2\left(M_C\widetilde{\boldsymbol{D}}_h^n,\delta_\tau\overline{\boldsymbol{E}}_h^n\right).
\end{aligned}
\tag{3.20}
$$

Multiplying (3.20) by $\frac{2}{\tau}$, we can rewrite (3.20) as:

$$
\begin{aligned}
&\frac{||\delta_\tau\boldsymbol{D}_h^{n+\frac{1}{2}}||^2-||\delta_\tau\boldsymbol{D}_h^{n-\frac{1}{2}}||^2}{\tau}+\frac{||M_C^{\frac{1}{2}}\boldsymbol{D}_h^{n+1}||^2-||M_C^{\frac{1}{2}}\boldsymbol{D}_h^{n-1}||^2}{2\tau}\\
&+\varepsilon_0\lambda_2\frac{||M_A^{-\frac{1}{2}}\delta_\tau^2\boldsymbol{E}_h^n||^2-||M_A^{-\frac{1}{2}}\delta_\tau^2\boldsymbol{E}_h^{n-1}||^2}{\tau}\\
&+\varepsilon_0\lambda_2\omega_p^2\frac{||M_A^{-\frac{1}{2}}\delta_\tau\boldsymbol{E}_h^{n+\frac{1}{2}}||^2-||M_A^{-\frac{1}{2}}\delta_\tau\boldsymbol{E}_h^{n-\frac{3}{2}}||^2}{2\tau}\\
&+\frac{1}{\mu_0\mu}\cdot\frac{||\nabla\times\delta_\tau\overline{\boldsymbol{E}}_h^n||^2-||\nabla\times\delta_\tau\overline{\boldsymbol{E}}_h^{n-1}||^2}{\tau}\\
&+\varepsilon_0\lambda_2\omega_p^2\frac{||M_A^{-\frac{1}{2}}\delta_\tau\boldsymbol{E}_h^{n+\frac{1}{2}}||^2-||M_A^{-\frac{1}{2}}\delta_\tau\boldsymbol{E}_h^{n-\frac{1}{2}}||^2}{\tau}\\
&+\varepsilon_0\lambda_2\omega_p^4\frac{||M_A^{-\frac{1}{2}}\boldsymbol{E}_h^{n+1}||^2-||M_A^{-\frac{1}{2}}\boldsymbol{E}_h^{n-1}||^2}{2\tau}\\
&+\frac{\omega_p^2}{\mu_0\mu}\cdot\frac{||\nabla\times\overline{\boldsymbol{E}}_h^{n+\frac{1}{2}}||^2-||\nabla\times\overline{\boldsymbol{E}}_h^{n-\frac{1}{2}}||^2}{\tau}\\
=\ &2\varepsilon_0\lambda_2\left(M_A^{-1}\delta_\tau^2\boldsymbol{E}_h^n+\omega_p^2M_A^{-1}\widetilde{\boldsymbol{E}}_h^n,\delta_\tau\overline{\boldsymbol{D}}_h^n\right)\\
&\quad+2(M_C\delta_\tau\widetilde{\boldsymbol{D}}_h^{n-\frac{1}{2}},\delta_\tau^2\overline{\boldsymbol{E}}_h^{n-\frac{1}{2}})+2\omega_p^2\left(M_C\widetilde{\boldsymbol{D}}_h^n,\delta_\tau\overline{\boldsymbol{E}}_h^n\right),
\end{aligned}
\tag{3.21}
$$

which has really the same form (in a discrete sense) as (2.23).

Now, summing up (3.21) multiplied by τ from $n = 1$ to any $m \geq 2$, and using notation ENG_{cn} defined in (3.8), we obtain

$$ENG_{cn}(m) - ENG_{cn}(0) = \tau \sum_{n=1}^{m} 2\varepsilon_0\lambda_2 \left(M_A^{-1}\delta_\tau^2 \boldsymbol{E}_h^n + \omega_p^2 M_A^{-1} \widetilde{\boldsymbol{E}}_h^n, \delta_\tau \overline{\boldsymbol{D}}_h^n \right)$$
$$+ \tau \sum_{n=1}^{m} 2(M_C \delta_\tau \widetilde{\boldsymbol{D}}_h^{n-\frac{1}{2}}, \delta_\tau^2 \overline{\boldsymbol{E}}_h^{n-\frac{1}{2}}) + \tau \sum_{n=1}^{m} 2\omega_p^2 \left(M_C \widetilde{\boldsymbol{D}}_h^n, \delta_\tau \overline{\boldsymbol{E}}_h^n \right). \tag{3.22}$$

(V). Now, we just need to bound those RHS terms of (3.22) and use the discrete Gronwall inequality given in Lemma 3.1 to conclude the proof. To see clearly, below we present the estimate for those RHS terms of (3.22) one by one.

Using the following inequalities

$$2ab \leq a^2 + b^2, \quad |\frac{1}{2}(a+b)|^2 \leq \frac{1}{2}(a^2+b^2), \tag{3.23}$$

we have

$$\tau \sum_{n=1}^{m} 2\varepsilon_0\lambda_2 (M_A^{-1}\delta_\tau^2 \boldsymbol{E}_h^n, \delta_\tau \overline{\boldsymbol{D}}_h^n) \leq \tau \sum_{n=1}^{m} 2\varepsilon_0\lambda_2 ||M_A^{-\frac{1}{2}}\delta_\tau^2 \boldsymbol{E}_h^n|| \cdot ||M_A^{-\frac{1}{2}}||_2 ||\delta_\tau \overline{\boldsymbol{D}}_h^n||$$
$$\leq \tau\sqrt{\varepsilon_0\lambda_2}||M_A^{-\frac{1}{2}}||_2 \sum_{n=1}^{m} 2\left[\varepsilon_0\lambda_2||M_A^{-\frac{1}{2}}\delta_\tau^2 \boldsymbol{E}_h^n||^2 + \frac{1}{2}(||\delta_\tau \boldsymbol{D}_h^{n+\frac{1}{2}}||^2 + ||\delta_\tau \boldsymbol{D}_h^{n-\frac{1}{2}}||^2)\right]. \tag{3.24}$$

By the same argument, we have

$$\tau \sum_{n=1}^{m} 2\varepsilon_0\lambda_2 (\omega_p^2 M_A^{-1} \widetilde{\boldsymbol{E}}_h^n, \delta_\tau \overline{\boldsymbol{D}}_h^n) \leq \tau \sum_{n=1}^{m} 2\varepsilon_0\lambda_2\omega_p^2 ||M_A^{-\frac{1}{2}} \widetilde{\boldsymbol{E}}_h^n|| \cdot ||M_A^{-\frac{1}{2}}||_2 ||\delta_\tau \overline{\boldsymbol{D}}_h^n||$$
$$\leq \tau\sqrt{\varepsilon_0\lambda_2}||M_A^{-\frac{1}{2}}||_2 \sum_{n=1}^{m} \left(\varepsilon_0\lambda_2\omega_p^4 ||M_A^{-\frac{1}{2}} \widetilde{\boldsymbol{E}}_h^n||^2 + ||\delta_\tau \overline{\boldsymbol{D}}_h^n||^2 \right)$$
$$\leq \tau\sqrt{\varepsilon_0\lambda_2}||M_A^{-\frac{1}{2}}||_2 \sum_{n=1}^{m} \left[\frac{\varepsilon_0\lambda_2\omega_p^4}{2} \left(||M_A^{-\frac{1}{2}} \boldsymbol{E}_h^{n+1}||^2 + ||M_A^{-\frac{1}{2}} \boldsymbol{E}_h^{n-1}||^2 \right) \right.$$
$$\left. + \frac{1}{2}(||\delta_\tau \boldsymbol{D}_h^{n+\frac{1}{2}}||^2 + ||\delta_\tau \boldsymbol{D}_h^{n-\frac{1}{2}}||^2) \right], \tag{3.25}$$

$$\tau \sum_{n=1}^{m} 2(M_C \delta_\tau \widetilde{\boldsymbol{D}}_h^{n-\frac{1}{2}}, \delta_\tau^2 \overline{\boldsymbol{E}}_h^{n-\frac{1}{2}}) = \tau \sum_{n=1}^{m} 2(M_A^{-1} M_B \delta_\tau \widetilde{\boldsymbol{D}}_h^{n-\frac{1}{2}}, \delta_\tau^2 \overline{\boldsymbol{E}}_h^{n-\frac{1}{2}})$$
$$\leq \tau \sum_{n=1}^{m} \frac{2||M_A^{-\frac{1}{2}} M_B||_2}{\sqrt{\varepsilon_0\lambda_2}} ||\delta_\tau \widetilde{\boldsymbol{D}}_h^{n-\frac{1}{2}}|| \cdot \sqrt{\varepsilon_0\lambda_2}||M_A^{-\frac{1}{2}}\delta_\tau^2 \overline{\boldsymbol{E}}_h^{n-\frac{1}{2}}||$$

$$\leq \tau \cdot \frac{||M_A^{-\frac{1}{2}} M_B||_2}{\sqrt{\varepsilon_0 \lambda_2}} \sum_{n=1}^{m} \left(||\delta_\tau \widetilde{\boldsymbol{D}}_h^{n-\frac{1}{2}}||^2 + \varepsilon_0 \lambda_2 ||M_A^{-\frac{1}{2}} \delta_\tau^2 \overline{\boldsymbol{E}}_h^{n-\frac{1}{2}}||^2 \right)$$

$$\leq \tau \cdot \frac{||M_A^{-\frac{1}{2}} M_B||_2}{\sqrt{\varepsilon_0 \lambda_2}} \sum_{n=1}^{m} \left[\frac{1}{2} (||\delta_\tau \boldsymbol{D}_h^{n+\frac{1}{2}}||^2 + ||\delta_\tau \boldsymbol{D}_h^{n-\frac{3}{2}}||^2) + \frac{\varepsilon_0 \lambda_2}{2} (||M_A^{-\frac{1}{2}} \delta_\tau^2 \overline{\boldsymbol{E}}_h^{n}||^2 + ||M_A^{-\frac{1}{2}} \delta_\tau^2 \overline{\boldsymbol{E}}_h^{n-1}||^2) \right], \tag{3.26}$$

and

$$\tau \sum_{n=1}^{m} 2\omega_p^2 (M_C \widetilde{\boldsymbol{D}}_h^n, \delta_\tau \overline{\boldsymbol{E}}_h^n) = \tau \sum_{n=1}^{m} 2\omega_p^2 (M_C^{\frac{1}{2}} \widetilde{\boldsymbol{D}}_h^n, M_C^{\frac{1}{2}} M_A^{\frac{1}{2}} M_A^{-\frac{1}{2}} \delta_\tau \overline{\boldsymbol{E}}_h^n)$$

$$\leq \tau \sum_{n=1}^{m} 2\omega_p^2 ||M_C^{\frac{1}{2}} \widetilde{\boldsymbol{D}}_h^n|| \cdot ||M_C^{\frac{1}{2}} M_A^{\frac{1}{2}}||_2 ||M_A^{-\frac{1}{2}} \delta_\tau \overline{\boldsymbol{E}}_h^n||$$

$$\leq \tau \frac{\omega_p ||M_C^{\frac{1}{2}} M_A^{\frac{1}{2}}||_2}{\sqrt{\varepsilon_0 \lambda_2}} \sum_{n=1}^{m} \left(||M_C^{\frac{1}{2}} \widetilde{\boldsymbol{D}}_h^n||^2 + \varepsilon_0 \lambda_2 \omega_p^2 ||M_A^{-\frac{1}{2}} \delta_\tau \overline{\boldsymbol{E}}_h^n||^2 \right)$$

$$\leq \tau \frac{\omega_p ||M_C^{\frac{1}{2}} M_A^{\frac{1}{2}}||_2}{\sqrt{\varepsilon_0 \lambda_2}} \sum_{n=1}^{m} \left[\frac{1}{2} (||M_C^{\frac{1}{2}} \boldsymbol{D}_h^{n+1}||^2 + ||M_C^{\frac{1}{2}} \boldsymbol{D}_h^{n-1}||^2) + \frac{\varepsilon_0 \lambda_2 \omega_p^2}{2} (||M_A^{-\frac{1}{2}} \delta_\tau \boldsymbol{E}_h^{n+\frac{1}{2}}||^2 + ||M_A^{-\frac{1}{2}} \delta_\tau \boldsymbol{E}_h^{n-\frac{1}{2}}||^2) \right]. \tag{3.27}$$

Substituting the estimates (3.24), (3.25), (3.26), and (3.27) into (3.22), and choosing τ such that the coefficients of $\delta_\tau \boldsymbol{D}_h^{m+\frac{1}{2}}$, $\delta_\tau^2 \boldsymbol{E}_h^m$, $\boldsymbol{E}_h^{m+1}$, and $\delta_\tau \boldsymbol{E}_h^{m+\frac{1}{2}}$ on the RHS of (3.22) are smaller than the corresponding LHS terms, such as

$$\tau (\sqrt{\varepsilon_0 \lambda_2} ||M_A^{-\frac{1}{2}}||_2 + \frac{||M_A^{-\frac{1}{2}} M_B||_2}{2\sqrt{\varepsilon_0 \lambda_2}}) \leq \frac{1}{2},$$

$$\tau \frac{\sqrt{\varepsilon_0 \lambda_2} ||M_A^{-\frac{1}{2}}||_2}{2} \leq \frac{1}{4}, \quad \tau \frac{\omega_p ||M_C^{\frac{1}{2}} M_A^{\frac{1}{2}}||_2}{2\sqrt{\varepsilon_0 \lambda_2}} \leq \frac{1}{2}, \tag{3.28}$$

which is equivalent to (3.9), we obtain

$$\frac{1}{2} ENG_{cn}(m) - ENG_{cn}(0) \leq \frac{\tau}{2} \sum_{n=0}^{m-1} ENG_{cn}(n). \tag{3.29}$$

Applying the discrete Gronwall inequality given in Lemma 3.1 to (3.29), we complete the proof. □

4 The leap-frog scheme and its analysis

Now, we can construct a leap-frog (LF) scheme for solving (2.1)–(2.3): For $n \geq 0$ find $H_h^{n+\frac{1}{2}} \in U_h$, $\boldsymbol{D}_h^{n+1}$, $\boldsymbol{E}_h^{n+1} \in \boldsymbol{V}_h^0$, such that

$$\left(\delta_\tau \boldsymbol{D}_h^{n+\frac{1}{2}}, \boldsymbol{\phi}_h\right) = (H_h^{n+\frac{1}{2}}, \nabla \times \boldsymbol{\phi}_h), \tag{4.1}$$

$$\varepsilon_0 \lambda_2 \left(M_A^{-1} \delta_\tau^2 \boldsymbol{E}_h^n + \omega_p^2 M_A^{-1} \widetilde{\boldsymbol{E}}_h^n, \boldsymbol{\phi}_h\right) = \left(\delta_\tau^2 \boldsymbol{D}_h^n + M_C \widetilde{\boldsymbol{D}}_h^n, \boldsymbol{\phi}_h\right), \tag{4.2}$$

$$\mu_0 \mu \left(\delta_\tau H_h^n, \psi_h\right) = -(\nabla \times \boldsymbol{E}_h^n, \psi_h), \tag{4.3}$$

hold true for any $\boldsymbol{\phi}_h \in \boldsymbol{V}_h^0$ and $\psi_h \in U_h$.

The needed initial approximations $H_h^{-\frac{1}{2}}$, $\boldsymbol{D}_h^{-1}$, $\boldsymbol{D}_h^0$, $\boldsymbol{E}_h^{-1}$, $\boldsymbol{E}_h^0$ can be obtained from discretising the given initial conditions (2.7) as follows:

$$\boldsymbol{D}_h^0 = \Pi_c \boldsymbol{D}_0, \quad \boldsymbol{E}_h^0 = \Pi_c \boldsymbol{E}_0, \quad \overline{H}_h^0 := \frac{H_h^{\frac{1}{2}} + H_h^{-\frac{1}{2}}}{2} = \Pi_2 H_0, \tag{4.4}$$

$$\delta_{2\tau} \boldsymbol{D}_h^0 := \frac{\boldsymbol{D}_h^1 - \boldsymbol{D}_h^{-1}}{2\tau} = \Pi_c \boldsymbol{D}_1, \quad \delta_{2\tau} \boldsymbol{E}_h^0 := \frac{\boldsymbol{E}_h^1 - \boldsymbol{E}_h^{-1}}{2\tau} = \Pi_c \boldsymbol{E}_1. \tag{4.5}$$

The implementation of leap-frog scheme is quite simple. At each time step, we first solve (4.3) for $H_h^{n+\frac{1}{2}}$, then solve for $\boldsymbol{D}_h^{n+1}$ from (4.1), and finally update $\boldsymbol{E}_h^{n+1}$ from (4.2). We like to remark that in the first time step (when $n = 0$), we have to couple the initial conditions (4.4)-(4.5) with the scheme. More specifically, we first solve for $H_h^{\frac{1}{2}}$ from

$$(H_h^{\frac{1}{2}}, \psi_h) = (\Pi_2 H_0, \psi_h) - \frac{\tau}{2\mu_0 \mu}(\nabla \times \boldsymbol{E}_h^0, \psi_h).$$

Then, we can obtain $\boldsymbol{D}_h^1$ from

$$(\boldsymbol{D}_h^1, \boldsymbol{\phi}_h) = (\boldsymbol{D}_h^0, \boldsymbol{\phi}_h) + \tau (H_h^{\frac{1}{2}}, \nabla \times \boldsymbol{\phi}_h).$$

After substitution of (4.5) into (4.2) with $n = 0$ and some algebra operations, we find that $\boldsymbol{E}_h^1$ can be obtained by solving the equation:

$$\begin{aligned} \varepsilon_0 \lambda_2 (2 + \tau^2 \omega_p^2)(\boldsymbol{E}_h^1, \boldsymbol{\phi}_h) &= \left(2\varepsilon_0 \lambda_2 \boldsymbol{E}_h^0 + \tau \varepsilon_0 \lambda_2 (2 + \tau^2 \omega_p^2) \Pi_c \boldsymbol{E}_1, \boldsymbol{\phi}_h\right) \\ &+ \left(2M_A(\boldsymbol{D}_h^1 - \boldsymbol{D}_h^0 - \tau \Pi_c \boldsymbol{D}_1) + \tau^2 M_B(\boldsymbol{D}_h^1 - \tau \Pi_c \boldsymbol{D}_1), \boldsymbol{\phi}_h\right). \end{aligned}$$

4.1 The stability analysis

In this section, we will present the stability analysis for the leap-frog scheme (4.1)–(4.3).

Denote the positive constant C_{inv} appearing in the standard inverse estimate:

$$||\nabla \times u_h|| \leq C_{inv} h^{-1} ||u_h||, \ \forall\, u_h \in \boldsymbol{V}_h. \tag{4.6}$$

Theorem 4.1 *For the FE solution* $(\boldsymbol{D}_h^{n+1}, \boldsymbol{E}_h^{n+1}, H_h^{n+\frac{1}{2}})$ *of the leap-frog scheme (4.1)–(4.3), suppose that the time step size satisfies the following constraint*

$$\tau \le \min\left\{1/\left(\sqrt{\varepsilon_0\lambda_2}||M_A^{-\frac{1}{2}}||_2 + \frac{||M_A^{-\frac{1}{2}}M_B||_2}{2\sqrt{\varepsilon_0\lambda_2}}\right),\ \frac{\sqrt{\varepsilon_0\lambda_2}}{\omega_p||M_C^{\frac{1}{2}}M_A^{\frac{1}{2}}||_2},\ \frac{h\sqrt{\mu_0\mu\varepsilon_0\lambda_2}}{C_{inv}||M_A^{\frac{1}{2}}||_2}\right\}, \tag{4.7}$$

then we have

$$ENG_{cn}(m) \le 4ENG_{cn}(0)\cdot\exp(4m\tau), \quad \forall\, m \ge 1.$$

Remark 4.2 Compared to the time step constraint (3.9) imposed on the Crank-Nicolson scheme, the current constraint (4.7) depends on the mesh size h and needs $\tau = O(h)$, which makes the leap-frog scheme a conditionally stable scheme.

Proof The proof closely follows the continuous case given for Theorem 2.1 and is quite similar to the proof established for the CN scheme. We will point out some significant differences during the following proof. To make our proof easy to follow, we divide the proof into several major parts also.

(I). Choosing $\boldsymbol{\phi}_h = \tau\delta_\tau\overline{\boldsymbol{D}}_h^n$ in (4.2), and noting that (4.2) is exactly the same as (3.3) in the CN scheme, hence we have (3.12), i.e.,

$$\begin{aligned}&\frac{1}{2}(||\delta_\tau\boldsymbol{D}_h^{n+\frac{1}{2}}||^2 - ||\delta_\tau\boldsymbol{D}_h^{n-\frac{1}{2}}||^2) + \frac{1}{4}(||M_C^{\frac{1}{2}}\boldsymbol{D}_h^{n+1}||^2 - ||M_C^{\frac{1}{2}}\boldsymbol{D}_h^{n-1}||^2)\\ &= \tau\varepsilon_0\lambda_2\left(M_A^{-1}\delta_\tau^2\boldsymbol{E}_h^n + \omega_p^2M_A^{-1}\widetilde{\boldsymbol{E}}_h^n, \delta_\tau\overline{\boldsymbol{D}}_h^n\right).\end{aligned} \tag{4.8}$$

(II). Since (4.2) is the same as (3.3) in the CN scheme, (3.13) holds true for the LF scheme also, i.e., we have

$$\begin{aligned}&\varepsilon_0\lambda_2\left(M_A^{-1}\frac{\delta_\tau^2\boldsymbol{E}_h^{n+1} - \delta_\tau^2\boldsymbol{E}_h^n}{\tau} + \omega_p^2M_A^{-1}\frac{\widetilde{\boldsymbol{E}}_h^{n+1} - \widetilde{\boldsymbol{E}}_h^n}{\tau}, \boldsymbol{\phi}_h\right)\\ &= \left(\frac{\delta_\tau^2\boldsymbol{D}_h^{n+1} - \delta_\tau^2\boldsymbol{D}_h^n}{\tau} + M_C\frac{\widetilde{\boldsymbol{D}}_h^{n+1} - \widetilde{\boldsymbol{D}}_h^n}{\tau}, \boldsymbol{\phi}_h\right).\end{aligned} \tag{4.9}$$

To estimate $(\frac{\delta_\tau^2\boldsymbol{D}_h^{n+1} - \delta_\tau^2\boldsymbol{D}_h^n}{\tau}, \boldsymbol{\phi}_h)$, using (4.1) and (4.3), we have

$$\begin{aligned}\left(\frac{\delta_\tau^2\boldsymbol{D}_h^{n+1} - \delta_\tau^2\boldsymbol{D}_h^n}{\tau}, \boldsymbol{\phi}_h\right) &= \left(\frac{(\delta_\tau\boldsymbol{D}_h^{n+\frac{3}{2}} - \delta_\tau\boldsymbol{D}_h^{n+\frac{1}{2}}) - (\delta_\tau\boldsymbol{D}_h^{n+\frac{1}{2}} - \delta_\tau\boldsymbol{D}_h^{n-\frac{1}{2}})}{\tau^2}, \boldsymbol{\phi}_h\right)\\ \overset{by(4.1)}{=} \left(\frac{(H_h^{n+\frac{3}{2}} - H_h^{n+\frac{1}{2}}) - (H_h^{n+\frac{1}{2}} - H_h^{n-\frac{1}{2}})}{\tau^2}, \nabla\times\boldsymbol{\phi}_h\right) &= \left(\frac{\delta_\tau H_h^{n+1} - \delta_\tau H_h^n}{\tau}, \nabla\times\boldsymbol{\phi}_h\right)\\ \overset{by(4.3)}{=} \frac{-1}{\mu_0\mu}\left(\frac{\nabla\times\boldsymbol{E}_h^{n+1} - \nabla\times\boldsymbol{E}_h^n}{\tau}, \nabla\times\boldsymbol{\phi}_h\right)&\\ = \frac{-1}{\mu_0\mu}\left(\nabla\times\delta_\tau\boldsymbol{E}_h^{n+\frac{1}{2}}, \nabla\times\boldsymbol{\phi}_h\right).&\end{aligned} \tag{4.10}$$

Choosing $\boldsymbol{\phi}_h = \tau\delta_\tau^2\overline{\boldsymbol{E}}_h^{n+\frac{1}{2}} = \delta_\tau\overline{\boldsymbol{E}}_h^{n+1} - \delta_\tau\overline{\boldsymbol{E}}_h^{n}$ in (4.10), we have

$$\left(\frac{\delta_\tau^2\boldsymbol{D}_h^{n+1}-\delta_\tau^2\boldsymbol{D}_h^{n}}{\tau},\boldsymbol{\phi}_h\right) = \frac{-1}{\mu_0\mu}\left(\nabla\times\delta_\tau\boldsymbol{E}_h^{n+\frac{1}{2}},\nabla\times(\delta_\tau\overline{\boldsymbol{E}}_h^{n+1}-\delta_\tau\overline{\boldsymbol{E}}_h^{n})\right)$$
$$= \frac{-1}{\mu_0\mu}\left(\nabla\times\delta_\tau\boldsymbol{E}_h^{n+\frac{1}{2}} - \nabla\times(\frac{\delta_\tau\overline{\boldsymbol{E}}_h^{n+1}+\delta_\tau\overline{\boldsymbol{E}}_h^{n}}{2}),\nabla\times(\delta_\tau\overline{\boldsymbol{E}}_h^{n+1}-\delta_\tau\overline{\boldsymbol{E}}_h^{n})\right)$$
$$-\frac{1}{2\mu_0\mu}(||\nabla\times\delta_\tau\overline{\boldsymbol{E}}_h^{n+1}||^2 - ||\nabla\times\delta_\tau\overline{\boldsymbol{E}}_h^{n}||^2). \tag{4.11}$$

To simplify the first term on the RHS of (4.11), we notice that

$$\left(\nabla\times\delta_\tau(\frac{\overline{\boldsymbol{E}}_h^{n+1}+\overline{\boldsymbol{E}}_h^{n}}{2}) - \nabla\times\delta_\tau\boldsymbol{E}_h^{n+\frac{1}{2}},\nabla\times(\delta_\tau\overline{\boldsymbol{E}}_h^{n+1}-\delta_\tau\overline{\boldsymbol{E}}_h^{n})\right)$$
$$= \left(\nabla\times\delta_\tau(\frac{\boldsymbol{E}_h^{n+\frac{3}{2}}+\boldsymbol{E}_h^{n+\frac{1}{2}}+\boldsymbol{E}_h^{n+\frac{1}{2}}+\boldsymbol{E}_h^{n-\frac{1}{2}}}{4} - \boldsymbol{E}_h^{n+\frac{1}{2}}),\nabla\times(\tau\delta_\tau^2\overline{\boldsymbol{E}}_h^{n+\frac{1}{2}})\right)$$
$$= \tau\left(\nabla\times\delta_\tau(\frac{\boldsymbol{E}_h^{n+\frac{3}{2}}-2\boldsymbol{E}_h^{n+\frac{1}{2}}+\boldsymbol{E}_h^{n-\frac{1}{2}}}{4}),\nabla\times\delta_\tau^2\overline{\boldsymbol{E}}_h^{n+\frac{1}{2}}\right)$$
$$= \tau^2\left(\nabla\times\delta_\tau(\frac{\delta_\tau\boldsymbol{E}_h^{n+1}-\delta_\tau\boldsymbol{E}_h^{n}}{4}),\nabla\times\delta_\tau^2\overline{\boldsymbol{E}}_h^{n+\frac{1}{2}}\right)$$
$$= \frac{\tau^2}{4}\left(\nabla\times(\delta_\tau^2\boldsymbol{E}_h^{n+1}-\delta_\tau^2\boldsymbol{E}_h^{n}),\nabla\times\delta_\tau^2(\frac{\boldsymbol{E}_h^{n+1}+\boldsymbol{E}_h^{n}}{2})\right)$$
$$= \frac{\tau^2}{8}\left(||\nabla\times\delta_\tau^2\boldsymbol{E}_h^{n+1}||^2 - ||\nabla\times\delta_\tau^2\boldsymbol{E}_h^{n}||^2\right). \tag{4.12}$$

Substituting the estimate (4.11) with the application of (4.12), and the identity (by using (3.16) and (3.17))

$$(\frac{\widetilde{\boldsymbol{E}}_h^{n+1}-\widetilde{\boldsymbol{E}}_h^{n}}{\tau},\delta_\tau\overline{\boldsymbol{E}}_h^{n+1}-\delta_\tau\overline{\boldsymbol{E}}_h^{n}) = \frac{1}{4}\left(||\delta_\tau\boldsymbol{E}_h^{n+\frac{3}{2}}||^2 - ||\delta_\tau\boldsymbol{E}_h^{n-\frac{1}{2}}||^2\right) \tag{4.13}$$

into (4.10), and then into (4.9) with $\boldsymbol{\phi}_h = \tau\delta_\tau^2\overline{\boldsymbol{E}}_h^{n+\frac{1}{2}}$, we obtain

$$\frac{\varepsilon_0\lambda_2}{2}(||M_A^{-\frac{1}{2}}\delta_\tau^2\boldsymbol{E}_h^{n+1}||^2 - ||M_A^{-\frac{1}{2}}\delta_\tau^2\boldsymbol{E}_h^{n}||^2)$$
$$+\frac{\varepsilon_0\lambda_2\omega_p^2}{4}(||M_A^{-\frac{1}{2}}\delta_\tau\boldsymbol{E}_h^{n+\frac{3}{2}}||^2 - ||M_A^{-\frac{1}{2}}\delta_\tau\boldsymbol{E}_h^{n-\frac{1}{2}}||^2)$$
$$+\frac{1}{2\mu_0\mu}(||\nabla\times\delta_\tau\overline{\boldsymbol{E}}_h^{n+1}||^2 - ||\nabla\times\delta_\tau\overline{\boldsymbol{E}}_h^{n}||^2)$$
$$= \frac{\tau^2}{8\mu_0\mu}(||\nabla\times\delta_\tau^2\boldsymbol{E}_h^{n+1}||^2 - ||\nabla\times\delta_\tau^2\boldsymbol{E}_h^{n}||^2) + \tau(M_C\delta_\tau\widetilde{\boldsymbol{D}}_h^{n+\frac{1}{2}},\delta_\tau^2\overline{\boldsymbol{E}}_h^{n+\frac{1}{2}}). \tag{4.14}$$

(III). Choosing $\boldsymbol{\phi}_h = \tau\delta_\tau \overline{\boldsymbol{E}}_h^n$ in (4.2), and by the same argument as (I), we have

$$\begin{aligned}&\frac{\varepsilon_0\lambda_2}{2}(||M_A^{-\frac{1}{2}}\delta_\tau \boldsymbol{E}_h^{n+\frac{1}{2}}||^2 - ||M_A^{-\frac{1}{2}}\delta_\tau \boldsymbol{E}_h^{n-\frac{1}{2}}||^2)\\&+\frac{\varepsilon_0\lambda_2\omega_p^2}{4}(||M_A^{-\frac{1}{2}}\boldsymbol{E}_h^{n+1}||^2 - ||M_A^{-\frac{1}{2}}\boldsymbol{E}_h^{n-1}||^2)\\=\ &\tau\left(\delta_\tau^2 \boldsymbol{D}_h^n + M_C\widetilde{\boldsymbol{D}}_h^n, \delta_\tau \overline{\boldsymbol{E}}_h^n\right). \qquad (4.15)\end{aligned}$$

To estimate the term $\delta_\tau^2 \boldsymbol{D}_h^n$ on the RHS of (4.15), by using (4.1) and (4.3), we obtain

$$\begin{aligned}&\tau(\delta_\tau^2 \boldsymbol{D}_h^n, \delta_\tau \overline{\boldsymbol{E}}_h^n) = (\delta_\tau \boldsymbol{D}_h^{n+\frac{1}{2}} - \delta_\tau \boldsymbol{D}_h^{n-\frac{1}{2}}, \delta_\tau \overline{\boldsymbol{E}}_h^n)\\\overset{by(4.1)}{=}\ &(H_h^{n+\frac{1}{2}} - H_h^{n-\frac{1}{2}}, \nabla\times\delta_\tau \overline{\boldsymbol{E}}_h^n) = \tau(\delta_\tau H_h^n, \nabla\times\delta_\tau \overline{\boldsymbol{E}}_h^n)\\\overset{by(4.3)}{=}\ &\frac{-\tau}{\mu_0\mu}(\nabla\times \boldsymbol{E}_h^n, \nabla\times\delta_\tau \overline{\boldsymbol{E}}_h^n)\\=\ &\frac{-1}{\mu_0\mu}\left(\nabla\times(\boldsymbol{E}_h^n - \frac{\overline{\boldsymbol{E}}_h^{n+\frac{1}{2}} + \overline{\boldsymbol{E}}_h^{n-\frac{1}{2}}}{2})\right.\\&\left.+\nabla\times\frac{\overline{\boldsymbol{E}}_h^{n+\frac{1}{2}} + \overline{\boldsymbol{E}}_h^{n-\frac{1}{2}}}{2}, \nabla\times(\overline{\boldsymbol{E}}_h^{n+\frac{1}{2}} - \overline{\boldsymbol{E}}_h^{n-\frac{1}{2}})\right)\\=\ &\frac{-1}{2\mu_0\mu}\left(||\nabla\times\overline{\boldsymbol{E}}_h^{n+\frac{1}{2}}||^2 - ||\nabla\times\overline{\boldsymbol{E}}_h^{n-\frac{1}{2}}||^2\right)\\&+\frac{1}{\mu_0\mu}\left(\nabla\times\frac{\overline{\boldsymbol{E}}_h^{n+\frac{1}{2}} + \overline{\boldsymbol{E}}_h^{n-\frac{1}{2}} - 2\boldsymbol{E}^n}{2}, \nabla\times(\overline{\boldsymbol{E}}_h^{n+\frac{1}{2}} - \overline{\boldsymbol{E}}_h^{n-\frac{1}{2}})\right). \qquad (4.16)\end{aligned}$$

The second RHS term of (4.16) can be simplified further as (similar to (4.12))

$$\begin{aligned}&\frac{1}{\mu_0\mu}\left(\nabla\times\frac{\overline{\boldsymbol{E}}_h^{n+\frac{1}{2}} + \overline{\boldsymbol{E}}_h^{n-\frac{1}{2}} - 2\boldsymbol{E}^n}{2}, \nabla\times(\overline{\boldsymbol{E}}_h^{n+\frac{1}{2}} - \overline{\boldsymbol{E}}_h^{n-\frac{1}{2}})\right)\\=\ &\frac{\tau}{4\mu_0\mu}\left(\nabla\times(\delta_\tau \boldsymbol{E}_h^{n+\frac{1}{2}} - \delta_\tau \boldsymbol{E}_h^{n-\frac{1}{2}}), \tau\nabla\times\delta_\tau \overline{\boldsymbol{E}}_h^n\right)\\=\ &\frac{\tau^2}{8\mu_0\mu}\left(||\nabla\times\delta_\tau \boldsymbol{E}_h^{n+\frac{1}{2}}||^2 - ||\nabla\times\delta_\tau \boldsymbol{E}_h^{n-\frac{1}{2}}||^2\right). \qquad (4.17)\end{aligned}$$

Substituting (4.17) into (4.16), then into (4.15), we have

$$\begin{aligned}&\frac{\varepsilon_0\lambda_2}{2}(||M_A^{-\frac{1}{2}}\delta_\tau \boldsymbol{E}_h^{n+\frac{1}{2}}||^2 - ||M_A^{-\frac{1}{2}}\delta_\tau \boldsymbol{E}_h^{n-\frac{1}{2}}||^2) + \frac{\varepsilon_0\lambda_2\omega_p^2}{4}(||M_A^{-\frac{1}{2}}\boldsymbol{E}_h^{n+1}||^2 - ||M_A^{-\frac{1}{2}}\boldsymbol{E}_h^{n-1}||^2)\\&+\frac{1}{2\mu_0\mu}\left(||\nabla\times\overline{\boldsymbol{E}}_h^{n+\frac{1}{2}}||^2 - ||\nabla\times\overline{\boldsymbol{E}}_h^{n-\frac{1}{2}}||^2\right)\\=\ &\frac{\tau^2}{8\mu_0\mu}\left(||\nabla\times\delta_\tau \boldsymbol{E}_h^{n+\frac{1}{2}}||^2 - ||\nabla\times\delta_\tau \boldsymbol{E}_h^{n-\frac{1}{2}}||^2\right) + \tau\left(M_C\widetilde{\boldsymbol{D}}_h^n, \delta_\tau \overline{\boldsymbol{E}}_h^n\right). \qquad (4.18)\end{aligned}$$

(IV). Since term $\delta_\tau \widetilde{\boldsymbol{D}}_h^{n+\frac{1}{2}}$ in (4.14) can not be controlled by the like LHS term of (4.8), we add (4.14) with all n's reduced by one to (4.8), and (4.18) multiplied by ω_p^2 (to get the same coefficient for $||M_A^{-\frac{1}{2}}\delta_\tau \boldsymbol{E}_h^{n+\frac{1}{2}}||^2$), we obtain

$$\begin{aligned}
&\frac{1}{2}(||\delta_\tau \boldsymbol{D}_h^{n+\frac{1}{2}}||^2 - ||\delta_\tau \boldsymbol{D}_h^{n-\frac{1}{2}}||^2) + \frac{1}{4}(||M_C^{\frac{1}{2}}\boldsymbol{D}_h^{n+1}||^2 - ||M_C^{\frac{1}{2}}\boldsymbol{D}_h^{n-1}||^2) \\
&+\frac{\varepsilon_0\lambda_2}{2}(||M_A^{-\frac{1}{2}}\delta_\tau^2 \boldsymbol{E}_h^n||^2 - ||M_A^{-\frac{1}{2}}\delta_\tau^2 \boldsymbol{E}_h^{n-1}||^2) \\
&+\frac{\varepsilon_0\lambda_2\omega_p^2}{4}(||M_A^{-\frac{1}{2}}\delta_\tau \boldsymbol{E}_h^{n+\frac{1}{2}}||^2 - ||M_A^{-\frac{1}{2}}\delta_\tau \boldsymbol{E}_h^{n-\frac{3}{2}}||^2) \\
&+\frac{1}{2\mu_0\mu}(||\nabla\times\delta_\tau \overline{\boldsymbol{E}}_h^n||^2 - ||\nabla\times\delta_\tau \overline{\boldsymbol{E}}_h^{n-1}||^2) \\
&+\frac{\varepsilon_0\lambda_2\omega_p^2}{2}(||M_A^{-\frac{1}{2}}\delta_\tau \boldsymbol{E}_h^{n+\frac{1}{2}}||^2 - ||M_A^{-\frac{1}{2}}\delta_\tau \boldsymbol{E}_h^{n-\frac{1}{2}}||^2) \\
&+\frac{\varepsilon_0\lambda_2\omega_p^4}{4}(||M_A^{-\frac{1}{2}}\boldsymbol{E}_h^{n+1}||^2 - ||M_A^{-\frac{1}{2}}\boldsymbol{E}_h^{n-1}||^2) \\
&+\frac{\omega_p^2}{2\mu_0\mu}\left(||\nabla\times\overline{\boldsymbol{E}}_h^{n+\frac{1}{2}}||^2 - ||\nabla\times\overline{\boldsymbol{E}}_h^{n-\frac{1}{2}}||^2\right) \\
=\ &\frac{\tau^2}{8\mu_0\mu}(||\nabla\times\delta_\tau^2 \boldsymbol{E}_h^n||^2 - ||\nabla\times\delta_\tau^2 \boldsymbol{E}_h^{n-1}||^2) \\
&+\frac{\tau^2\omega_p^2}{8\mu_0\mu}\left(||\nabla\times\delta_\tau \boldsymbol{E}_h^{n+\frac{1}{2}}||^2 - ||\nabla\times\delta_\tau \boldsymbol{E}_h^{n-\frac{1}{2}}||^2\right) \\
&\quad+\tau\varepsilon_0\lambda_2\left(M_A^{-1}\delta_\tau^2 \boldsymbol{E}_h^n + \omega_p^2 M_A^{-1}\widetilde{\boldsymbol{E}}_h^n, \delta_\tau \overline{\boldsymbol{D}}_h^n\right) \\
&\quad+\tau(M_C\delta_\tau \widetilde{\boldsymbol{D}}_h^{n-\frac{1}{2}}, \delta_\tau^2 \overline{\boldsymbol{E}}_h^{n-\frac{1}{2}}) + \tau\omega_p^2\left(M_C\widetilde{\boldsymbol{D}}_h^n, \delta_\tau \overline{\boldsymbol{E}}_h^n\right).
\end{aligned} \tag{4.19}$$

Comparing (4.19) to (3.20) obtained for the CN scheme, we amazingly see that (4.19) contains exactly the same terms as (3.20) except the first two extra RHS terms! We will show that these two extra terms cause the LF scheme to be conditionally stability, i.e., the time step is constrained by the mesh size.

Now, multiplying (4.19) by 2, then summing up the result from $n = 1$ to any $m \geq 2$, and using notation ENG_{cn} defined in (3.8), we obtain

$$\begin{aligned}
&ENG_{cn}(m) - ENG_{cn}(0) \\
=\ &\frac{\tau^2}{4\mu_0\mu}(||\nabla\times\delta_\tau^2 \boldsymbol{E}_h^m||^2 - ||\nabla\times\delta_\tau^2 \boldsymbol{E}_h^0||^2) + \frac{\tau^2\omega_p^2}{4\mu_0\mu}\left(||\nabla\times\delta_\tau \boldsymbol{E}_h^{m+\frac{1}{2}}||^2 - ||\nabla\times\delta_\tau \boldsymbol{E}_h^{\frac{1}{2}}||^2\right) \\
&+\tau\sum_{n=1}^m 2\varepsilon_0\lambda_2\left(M_A^{-1}\delta_\tau^2 \boldsymbol{E}_h^n + \omega_p^2 M_A^{-1}\widetilde{\boldsymbol{E}}_h^n, \delta_\tau \overline{\boldsymbol{D}}_h^n\right) \\
&+\tau\sum_{n=1}^m 2(M_C\delta_\tau \widetilde{\boldsymbol{D}}_h^{n-\frac{1}{2}}, \delta_\tau^2 \overline{\boldsymbol{E}}_h^{n-\frac{1}{2}}) + \tau\sum_{n=1}^m 2\omega_p^2\left(M_C\widetilde{\boldsymbol{D}}_h^n, \delta_\tau \overline{\boldsymbol{E}}_h^n\right).
\end{aligned} \tag{4.20}$$

(V). Now, we just need to bound the first two RHS terms of (4.20), since the rest of RHS terms can be bounded in exactly the same ways as the CN scheme.

By using the inverse estimate (4.6), we have

$$\begin{aligned}
&\frac{\tau^2}{4\mu_0\mu}(||\nabla\times\delta_\tau^2\boldsymbol{E}_h^m||^2-||\nabla\times\delta_\tau^2\boldsymbol{E}_h^0||^2)\\
&\leq \frac{\tau^2}{4\mu_0\mu}\cdot(C_{inv}h^{-1})^2(||\delta_\tau^2\boldsymbol{E}_h^m||^2+||\delta_\tau^2\boldsymbol{E}_h^0||^2)\\
&= \frac{\tau^2}{4\mu_0\mu}\cdot(C_{inv}h^{-1})^2(||M_A^{\frac{1}{2}}M_A^{-\frac{1}{2}}\delta_\tau^2\boldsymbol{E}_h^m||^2+||M_A^{\frac{1}{2}}M_A^{-\frac{1}{2}}\delta_\tau^2\boldsymbol{E}_h^0||^2)\\
&\leq \frac{(\tau C_{inv}h^{-1}||M_A^{\frac{1}{2}}||_2)^2}{4\mu_0\mu\varepsilon_0\lambda_2}\left(\varepsilon_0\lambda_2||M_A^{-\frac{1}{2}}\delta_\tau^2\boldsymbol{E}_h^m||^2+\varepsilon_0\lambda_2||M_A^{-\frac{1}{2}}\delta_\tau^2\boldsymbol{E}_h^0||^2\right),
\end{aligned} \tag{4.21}$$

and

$$\begin{aligned}
&\frac{\tau^2\omega_p^2}{4\mu_0\mu}\left(||\nabla\times\delta_\tau\boldsymbol{E}_h^{m+\frac{1}{2}}||^2-||\nabla\times\delta_\tau\boldsymbol{E}_h^{\frac{1}{2}}||^2\right)\\
&\leq \frac{\tau^2\omega_p^2}{4\mu_0\mu}\cdot(C_{inv}h^{-1})^2\left(||\delta_\tau\boldsymbol{E}_h^{m+\frac{1}{2}}||^2+||\delta_\tau\boldsymbol{E}_h^{\frac{1}{2}}||^2\right)\\
&\leq \frac{(\tau C_{inv}h^{-1}||M_A^{\frac{1}{2}}||_2)^2}{4\mu_0\mu\varepsilon_0\lambda_2}\left(\varepsilon_0\lambda_2\omega_p^2||M_A^{-\frac{1}{2}}\delta_\tau\boldsymbol{E}_h^{m+\frac{1}{2}}||^2+\varepsilon_0\lambda_2\omega_p^2||M_A^{-\frac{1}{2}}\delta_\tau\boldsymbol{E}_h^{\frac{1}{2}}||^2\right).
\end{aligned} \tag{4.22}$$

Suppose that the time step size τ satisfies (3.28) and

$$\frac{(\tau C_{inv}h^{-1}||M_A^{\frac{1}{2}}||_2)^2}{4\mu_0\mu\varepsilon_0\lambda_2}\leq\frac{1}{4},\quad \text{or } \tau\leq\frac{h\sqrt{\mu_0\mu\varepsilon_0\lambda_2}}{C_{inv}||M_A^{\frac{1}{2}}||_2}, \tag{4.23}$$

which leads to (4.7), we obtain

$$\frac{1}{4}ENG_{cn}(m)-ENG_{cn}(0)\leq\frac{3\tau}{4}\sum_{n=0}^{m-1}ENG_{cn}(n). \tag{4.24}$$

Applying the discrete Gronwall inequality given in Lemma 3.1 to (4.24), we complete the proof. □

4.2 Convergence analysis

Furthermore, we denote the errors between the numerical solution $(\boldsymbol{D}_h^{n+1}, \boldsymbol{E}_h^{n+1}, H_h^{n+\frac{1}{2}})$ of (4.1)-(4.3) and the exact solution $(\boldsymbol{D}(\boldsymbol{x}, t_{n+1}), \boldsymbol{E}(\boldsymbol{x}, t_{n+1}), H(\boldsymbol{x}, t_{n+\frac{1}{2}}))$ of (2.1)–(2.3):

$$\begin{aligned}
&\boldsymbol{D}_h^{n+1}-\boldsymbol{D}(\boldsymbol{x},t_{n+1})=(\boldsymbol{D}_h^{n+1}-\Pi_c\boldsymbol{D}^{n+1})-(\boldsymbol{D}^{n+1}-\Pi_c\boldsymbol{D}^{n+1})=\boldsymbol{D}_{h\xi}^{n+1}-\boldsymbol{D}_{h\eta}^{n+1},\\
&\boldsymbol{E}_h^{n+1}-\boldsymbol{E}(\boldsymbol{x},t_{n+1})=(\boldsymbol{E}_h^{n+1}-\Pi_c\boldsymbol{E}^{n+1})-(\boldsymbol{E}^{n+1}-\Pi_c\boldsymbol{E}^{n+1})=\boldsymbol{E}_{h\xi}^{n+1}-\boldsymbol{E}_{h\eta}^{n+1},\\
&H_h^{n+\frac{1}{2}}-H(\boldsymbol{x},t_{n+\frac{1}{2}})=(H_h^{n+\frac{1}{2}}-\Pi_2H^{n+\frac{1}{2}})-(H^{n+\frac{1}{2}}-\Pi_2H^{n+\frac{1}{2}})=H_{h\xi}^{n+\frac{1}{2}}-H_{h\eta}^{n+\frac{1}{2}},
\end{aligned}$$

here and below for simplicity we just denote

$$\boldsymbol{D}^{n+1}=\boldsymbol{D}(\boldsymbol{x},t_{n+1}),\ \ \boldsymbol{E}^{n+1}=\boldsymbol{E}(\boldsymbol{x},t_{n+1}),\ \ H^{n+\frac{1}{2}}=H(\boldsymbol{x},t_{n+\frac{1}{2}}).$$

First, let us establish the error equations. From (2.1) and (4.1), we have

$$\begin{aligned}
&(\delta_\tau \boldsymbol{D}_{h\xi}^{n+\frac{1}{2}},\boldsymbol{\phi}_h)-(H_{h\xi}^{n+\frac{1}{2}},\nabla\times\boldsymbol{\phi}_h)\\
=\ &\left(\delta_\tau(\boldsymbol{D}_h^{n+\frac{1}{2}}-\Pi_c\boldsymbol{D}^{n+\frac{1}{2}}),\boldsymbol{\phi}_h\right)-(H_h^{n+\frac{1}{2}}-\Pi_2H^{n+\frac{1}{2}},\nabla\times\boldsymbol{\phi}_h)\\
\overset{by\ (4.1)\ and\ (2.1)}{=}\ &\left(\delta_\tau(I-\Pi_c)\boldsymbol{D}^{n+\frac{1}{2}}+\partial_t\boldsymbol{D}^{n+\frac{1}{2}}-\delta_\tau\boldsymbol{D}^{n+\frac{1}{2}},\boldsymbol{\phi}_h\right)\\
&-(\nabla\times H^{n+\frac{1}{2}},\boldsymbol{\phi}_h)+(\Pi_2H^{n+\frac{1}{2}},\nabla\times\boldsymbol{\phi}_h)\\
=\ &(\delta_\tau(I-\Pi_c)\boldsymbol{D}^{n+\frac{1}{2}},\boldsymbol{\phi}_h)+(\partial_t\boldsymbol{D}^{n+\frac{1}{2}}-\delta_\tau\boldsymbol{D}^{n+\frac{1}{2}},\boldsymbol{\phi}_h),
\end{aligned}\tag{4.25}$$

where in the last step we used integration by parts and the L^2 projection property $((I-\Pi_2)H^{n+\frac{1}{2}},\nabla\times\boldsymbol{\phi}_h)=0$, since $\nabla\times\boldsymbol{\phi}_h\in U_h$.

Similarly, from (4.2) and (2.2), we have

$$\begin{aligned}
&\varepsilon_0\lambda_2(M_A^{-1}\delta_\tau^2\boldsymbol{E}_{h\xi}^n+\omega_p^2M_A^{-1}\widetilde{\boldsymbol{E}}_{h\xi}^n,\boldsymbol{\varphi}_h)-(\delta_\tau^2\boldsymbol{D}_{h\xi}^n+M_C\widetilde{\boldsymbol{D}}_{h\xi}^n,\boldsymbol{\varphi}_h)\\
=\ &\varepsilon_0\lambda_2\left(M_A^{-1}\delta_\tau^2(\boldsymbol{E}_h^n-\Pi_c\boldsymbol{E}^n)+\omega_p^2M_A^{-1}(\widetilde{\boldsymbol{E}}_h^n-\Pi_c\widetilde{\boldsymbol{E}}^n),\boldsymbol{\varphi}_h\right)\\
&-\left(\delta_\tau^2(\boldsymbol{D}_h^n-\Pi_c\boldsymbol{D}^n)+M_C(\widetilde{\boldsymbol{D}}_h^n-\Pi_c\widetilde{\boldsymbol{D}}^n),\boldsymbol{\varphi}_h\right)\\
\overset{by\ (4.2),(2.2)}{=}\ &\varepsilon_0\lambda_2\left(M_A^{-1}\delta_\tau^2(I-\Pi_c)\boldsymbol{E}^n+M_A^{-1}(\partial_{t^2}\boldsymbol{E}^n-\delta_\tau^2\boldsymbol{E}^n),\boldsymbol{\varphi}_h\right)\\
&+\varepsilon_0\lambda_2\omega_p^2\left(M_A^{-1}(\boldsymbol{E}^n-\widetilde{\boldsymbol{E}}^n)+M_A^{-1}(I-\Pi_c)\widetilde{\boldsymbol{E}}^n,\boldsymbol{\varphi}_h\right)\\
&-\left(\delta_\tau^2(I-\Pi_c)\boldsymbol{D}^n+\partial_{t^2}\boldsymbol{D}^n-\delta_\tau^2\boldsymbol{D}^n,\boldsymbol{\varphi}_h\right)\\
&+\left(M_C(\boldsymbol{D}^n-\widetilde{\boldsymbol{D}}^n)+M_C(I-\Pi_c)\widetilde{\boldsymbol{D}}^n,\boldsymbol{\varphi}_h\right).
\end{aligned}\tag{4.26}$$

Finally, from (4.3) and (2.3), we obtain

$$\begin{aligned}
&\mu_0\mu\left(\delta_\tau H_{h\xi}^n,\psi_h\right)+(\nabla\times\boldsymbol{E}_{h\xi}^n,\psi_h)\\
=\ &\mu_0\mu\left(\delta_\tau(H_h^n-\Pi_2H^n),\psi_h\right)+(\nabla\times(\boldsymbol{E}_h^n-\Pi_c\boldsymbol{E}^n),\psi_h)\\
\overset{by\ (4.3),(2.3)}{=}\ &\mu_0\mu\left(\delta_\tau(I-\Pi_2)H^n+\partial_tH^n-\delta_\tau H^n,\psi_h\right)+(\nabla\times(I-\Pi_c)\boldsymbol{E}^n,\psi_h)\\
=\ &\mu_0\mu\left(\partial_tH^n-\delta_\tau H^n,\psi_h\right)+(\nabla\times(I-\Pi_c)\boldsymbol{E}^n,\psi_h),
\end{aligned}\tag{4.27}$$

where in the last step we used the L^2 projection property $((I-\Pi_2)H^n,\psi_h)=0$ for any $\psi_h\in U_h$.

In summary, we obtain the error equations given as follows:

$$\begin{aligned}
(I) \quad & (\delta_\tau \boldsymbol{D}_{h\xi}^{n+\frac{1}{2}}, \boldsymbol{\phi}_h) - (H_{h\xi}^{n+\frac{1}{2}}, \nabla \times \boldsymbol{\phi}_h) \\
& = (\delta_\tau (I - \Pi_c) \boldsymbol{D}^{n+\frac{1}{2}}, \boldsymbol{\phi}_h) + (\partial_t \boldsymbol{D}^{n+\frac{1}{2}} - \delta_\tau \boldsymbol{D}^{n+\frac{1}{2}}, \boldsymbol{\phi}_h), \qquad (4.28)\\
(II) \quad & \varepsilon_0 \lambda_2 (M_A^{-1} \delta_\tau^2 \boldsymbol{E}_{h\xi}^n + \omega_p^2 M_A^{-1} \widetilde{\boldsymbol{E}}_{h\xi}^n, \boldsymbol{\varphi}_h) - (\delta_\tau^2 \boldsymbol{D}_{h\xi}^n + M_C \widetilde{\boldsymbol{D}}_{h\xi}^n, \boldsymbol{\varphi}_h) \\
& = \varepsilon_0 \lambda_2 \left(M_A^{-1} \delta_\tau^2 (I - \Pi_c) \boldsymbol{E}^n + M_A^{-1} (\partial_{t^2} \boldsymbol{E}^n - \delta_\tau^2 \boldsymbol{E}^n), \boldsymbol{\varphi}_h \right) \\
& \quad + \varepsilon_0 \lambda_2 \omega_p^2 \left(M_A^{-1} (\boldsymbol{E}^n - \widetilde{\boldsymbol{E}}^n) + M_A^{-1} (I - \Pi_c) \widetilde{\boldsymbol{E}}^n, \boldsymbol{\varphi}_h \right) \qquad (4.29)\\
& \quad - \left(\delta_\tau^2 (I - \Pi_c) \boldsymbol{D}^n + \partial_{t^2} \boldsymbol{D}^n - \delta_\tau^2 \boldsymbol{D}^n, \boldsymbol{\varphi}_h \right) \\
& \quad + \left(M_C (\boldsymbol{D}^n - \widetilde{\boldsymbol{D}}^n) + M_C (I - \Pi_c) \widetilde{\boldsymbol{D}}^n, \boldsymbol{\varphi}_h \right), \\
(III) \quad & \mu_0 \mu \left(\delta_\tau H_{h\xi}^n, \psi_h \right) + (\nabla \times \boldsymbol{E}_{h\xi}^n, \psi_h) \\
& = \mu_0 \mu \left(\partial_t H^n - \delta_\tau H^n, \psi_h \right) + (\nabla \times (I - \Pi_c) \boldsymbol{E}^n, \psi_h), \qquad (4.30)
\end{aligned}$$

hold true for any $\boldsymbol{\phi}_h, \boldsymbol{\varphi}_h \in \boldsymbol{V}_h^0$ and $\psi_h \in U_h$.

Note that those LHS terms on the error equations (4.28)–(4.30) have exactly the same form as the leap-frog scheme (4.1)–(4.3), and the RHS terms are error terms incurred by interpolation and time approximations. Using the interpolation error estimate and Taylor expansion (cf. [30]), we can see that all the RHS terms have local errors $O(h^p + \tau^2)$, where $p \geq 1$ is the degree of the basis function in the FE spaces $\boldsymbol{V}_h^0$ and U_h.

Then, following the same procedure developed for the stability proof, we can prove the errors between the finite element solutions and their projections or interpolations given as:

$$\begin{aligned}
& ||\delta_\tau \boldsymbol{D}_{h\xi}^{n+\frac{1}{2}}||^2 + \frac{||M_C^{\frac{1}{2}} \boldsymbol{D}_{h\xi}^{n+1}||^2 + ||M_C^{\frac{1}{2}} \boldsymbol{D}_{h\xi}^n||^2}{2} + \varepsilon_0 \lambda_2 ||M_A^{-\frac{1}{2}} \delta_\tau^2 \boldsymbol{E}_{h\xi}^n||^2 \\
& \quad + \varepsilon_0 \lambda_2 \omega_p^2 \left[\frac{||M_A^{-\frac{1}{2}} \delta_\tau \boldsymbol{E}_{h\xi}^{n+\frac{1}{2}}||^2 + ||M_A^{-\frac{1}{2}} \delta_\tau \boldsymbol{E}_{h\xi}^{n-\frac{1}{2}}||^2}{2} + ||M_A^{-\frac{1}{2}} \delta_\tau \boldsymbol{E}_{h\xi}^{n+\frac{1}{2}}||^2 \right] \\
& \quad + \frac{1}{\mu_0 \mu} ||\nabla \times \delta_\tau \overline{\boldsymbol{E}}_{h\xi}^n||^2 + \varepsilon_0 \lambda_2 \omega_p^4 \left(\frac{||M_A^{-\frac{1}{2}} \boldsymbol{E}_{h\xi}^{n+1}||^2 + ||M_A^{-\frac{1}{2}} \boldsymbol{E}_{h\xi}^n||^2}{2} \right) \\
& + \frac{\omega_p^2}{\mu_0 \mu} ||\nabla \times \overline{\boldsymbol{E}}_{h\xi}^{n+\frac{1}{2}}||^2 \\
& \leq C(\tau^2 + h^p)^2. \qquad (4.31)
\end{aligned}$$

Now, using the triangle inequality, the estimate (4.31), the interpolation and projection error estimates (3.6)-(3.7), we have

$$\begin{aligned}
& ||\delta_\tau \boldsymbol{D}_h^{n+\frac{1}{2}} - \partial_t \boldsymbol{D}^{n+\frac{1}{2}}||^2 \\
= \ & ||\delta_\tau (\boldsymbol{D}_h^{n+\frac{1}{2}} - \Pi_c \boldsymbol{D}^{n+\frac{1}{2}}) + \delta_\tau ((\Pi_c - I) \boldsymbol{D}^{n+\frac{1}{2}}) + (\delta_\tau \boldsymbol{D}^{n+\frac{1}{2}} - \partial_t \boldsymbol{D}^{n+\frac{1}{2}})||^2
\end{aligned}$$

$$\leq 3\left(||\delta_\tau(\boldsymbol{D}_h^{n+\frac{1}{2}}-\Pi_c\boldsymbol{D}^{n+\frac{1}{2}})||^2+||\delta_\tau((\Pi_c-I)\boldsymbol{D}^{n+\frac{1}{2}})||^2+||\delta_\tau\boldsymbol{D}^{n+\frac{1}{2}}-\partial_t\boldsymbol{D}^{n+\frac{1}{2}}||^2\right)$$
$$\leq C(\tau^4+h^{2p})+\frac{C}{\tau}\int_{t_n}^{t_{n+1}}||(\Pi_c-I)\boldsymbol{D}||^2ds+C\tau^4||\partial_{t^3}\boldsymbol{D}||^2_{C([0,T];(L^2(\Omega))^3)}$$
$$\leq C(\tau^4+h^{2p})+Ch^{2p}||\partial_t\boldsymbol{D}||^2_{C([0,T];H^p(curl;\Omega))}+C\tau^4||\partial_{t^3}\boldsymbol{D}||^2_{C([0,T];(L^2(\Omega))^3)},$$

where we used the inequalities (cf. [27, Lemma 3.16])

$$\begin{aligned}||\delta_\tau u^n||^2 &:= ||\frac{u^{n+\frac{1}{2}}-u^{n-\frac{1}{2}}}{\tau}||^2\\ &\leq \frac{1}{\tau}\int_{t_{n-\frac{1}{2}}}^{t_{n+\frac{1}{2}}}||\partial_t u||^2ds, \quad \forall\, u\in H^1(0,T;L^2(\Omega)),\end{aligned} \tag{4.32}$$

and

$$|\delta_\tau\boldsymbol{D}^{n+\frac{1}{2}}-\partial_t\boldsymbol{D}^{n+\frac{1}{2}}|\leq C\tau^2\max_{0\leq t\leq T}|\partial_{t^3}\boldsymbol{D}|. \tag{4.33}$$

By the same technique, we can obtain the error estimate of the rest terms, which leads to the following optimal error estimate.

Theorem 4.3 *Suppose that the analytical solution* $(\boldsymbol{D},\boldsymbol{E},H)$ *of (2.1)–(2.3) are smooth enough and the time step size* τ *satisfies (4.7), then for any* $n\geq 1$ *we have*

$$\begin{aligned}&||\delta_\tau\boldsymbol{D}_h^{n+\frac{1}{2}}-\partial_t\boldsymbol{D}^{n+\frac{1}{2}}||^2+\frac{||M_C^{\frac{1}{2}}(\boldsymbol{D}_h^{n+1}-\boldsymbol{D}^{n+1})||^2+||M_C^{\frac{1}{2}}(\boldsymbol{D}_h^n-\boldsymbol{D}^n)||^2}{2}\\
&+\varepsilon_0\lambda_2||M_A^{-\frac{1}{2}}(\delta_\tau^2\boldsymbol{E}_h^n-\partial_{t^2}\boldsymbol{E}^n)||^2\\
&+\varepsilon_0\lambda_2\omega_p^2\left[\frac{||M_A^{-\frac{1}{2}}(\delta_\tau\boldsymbol{E}_h^{n+\frac{1}{2}}-\partial_t\boldsymbol{E}^{n+\frac{1}{2}})||^2+||M_A^{-\frac{1}{2}}(\delta_\tau\boldsymbol{E}_h^{n-\frac{1}{2}}-\partial_t\boldsymbol{E}^{n-\frac{1}{2}})||^2}{2}\right.\\
&\left.+||M_A^{-\frac{1}{2}}(\delta_\tau\boldsymbol{E}_h^{n+\frac{1}{2}}-\partial_t\boldsymbol{E}^{n+\frac{1}{2}}))||^2\right]\\
&+\frac{1}{\mu_0\mu}||\nabla\times(\delta_\tau\overline{\boldsymbol{E}}_h^n-\partial_t\overline{\boldsymbol{E}}^n))||^2\\
&+\varepsilon_0\lambda_2\omega_p^4\left(\frac{||M_A^{-\frac{1}{2}}(\boldsymbol{E}_h^{n+1}-\boldsymbol{E}^{n+1})||^2+||M_A^{-\frac{1}{2}}(\boldsymbol{E}_h^n-\boldsymbol{E}^n)||^2}{2}\right)\\
&+\frac{\omega_p^2}{\mu_0\mu}||\nabla\times(\overline{\boldsymbol{E}}_h^{n+\frac{1}{2}}-\overline{\boldsymbol{E}}^{n+\frac{1}{2}})||^2\leq C(\tau^2+h^p)^2,\end{aligned} \tag{4.34}$$

where the constant $C>0$ *is independent of* h *and* τ*, and* p *is the degree of the basis functions in* U_h *and* $\boldsymbol{V}_h$*.*

5 Numerical results

In this section, we first present some numerical results to justify the convergence result we proved for the leap-frog scheme, then we show that the interesting cloaking phenomenon can still be obtained by our new leap-frog scheme.

To test the convergence, we implement the leap-frog scheme (4.1)-(4.3) by using FEniCS [35] version 2016.1.0 installed under Ubuntu 14.04 on ThinkPad T440s Notebook (with 1.70-GHz CPU and 8-GB memory). Since an exact solution to the complicated model (2.1)–(2.3) is unknown, we just assume that the model has a solution for the electric field given as

$$\boldsymbol{E}(x, y, t) = \begin{pmatrix} E_x \\ E_y \end{pmatrix} = \begin{pmatrix} \cos(\omega x)\sin(\omega y) \\ -\sin(\omega x)\cos(\omega y) \end{pmatrix} e^{-\omega_f t}. \tag{5.1}$$

Then, we integrate (2.3) to obtain a magnetic solution

$$\begin{aligned} H(x, y, t) &= -\frac{1}{\mu_0\mu}\int^t \nabla\times\boldsymbol{E}dt = \frac{2}{\mu_0\mu}\int^t \cos(\omega x)\cos(\omega y)e^{-\omega_f t}dt \\ &= -\frac{2}{\mu_0\mu\omega_f}e^{-\omega_f t}\cos(\omega x)\cos(\omega y). \end{aligned} \tag{5.2}$$

Substituting (5.2) into (2.1), and integrating the result with respect to t, we obtain

$$\begin{aligned} \boldsymbol{D}(x, t, t) &= \int^t \nabla\times H dt = \int^t \frac{-2}{\mu_0\mu\omega_f}\begin{pmatrix} -\omega\cos(\omega x)\sin(\omega y) \\ \omega\sin(\omega x)\cos(\omega y) \end{pmatrix} e^{-\omega_f t}dt \\ &= \frac{-2\omega}{\mu_0\mu\omega_f^2}\begin{pmatrix} \cos(\omega x)\sin(\omega y) \\ -\sin(\omega x)\cos(\omega y) \end{pmatrix} e^{-\omega_f t}. \end{aligned} \tag{5.3}$$

To accommodate the above exact solutions, we have to add a source term $\boldsymbol{f}$ to the original governing equation (2.2) such that

$$\boldsymbol{f}(x, y, t) = \epsilon_0\lambda_2(\partial_t\boldsymbol{E} + \omega_p^2\boldsymbol{E}) - M_A\partial_{t^2}\boldsymbol{D} - M_B\boldsymbol{D}. \tag{5.4}$$

Hence, the implementation of (4.2) becomes

$$\varepsilon_0\lambda_2\left(\delta_\tau^2\boldsymbol{E}_h^n + \omega_p^2\widetilde{\boldsymbol{E}}_h^n\right) = M_A\delta_\tau^2\boldsymbol{D}_h^n + M_B\widetilde{\boldsymbol{D}}_h^n + \boldsymbol{f}(t_n). \tag{5.5}$$

In our simulation, we simply choose the physical domain Ω as the unit square, which is partitioned by a structured triangular mesh. A sample coarse mesh is shown in Fig. 1. To test the convergence rate, we use a sequence of uniformly refined meshes.

Example 1. For this test, we chose the physical parameters as follows:

$$\begin{aligned} H_1 &= 0.05,\ H_2 = 0.2,\ d = 0.2,\ \epsilon_0 = \mu_0 = \omega_f = \pi,\ \omega = 4\pi, \\ T &= 1e-4,\ \tau = 1e-6. \end{aligned}$$

The scheme (4.1), (5.5), and (4.3) is solved with the pth order Nédélec curl conforming edge element space $\boldsymbol{V}_h$ and the $(p-1)$th order L^2 finite element space U_h on triangular elements with $p = 1$ and $p = 2$. We solved this example on a series of uniformly refined $n\times n$ triangular meshes as Fig. 1. In Table 1, we presented the L^2

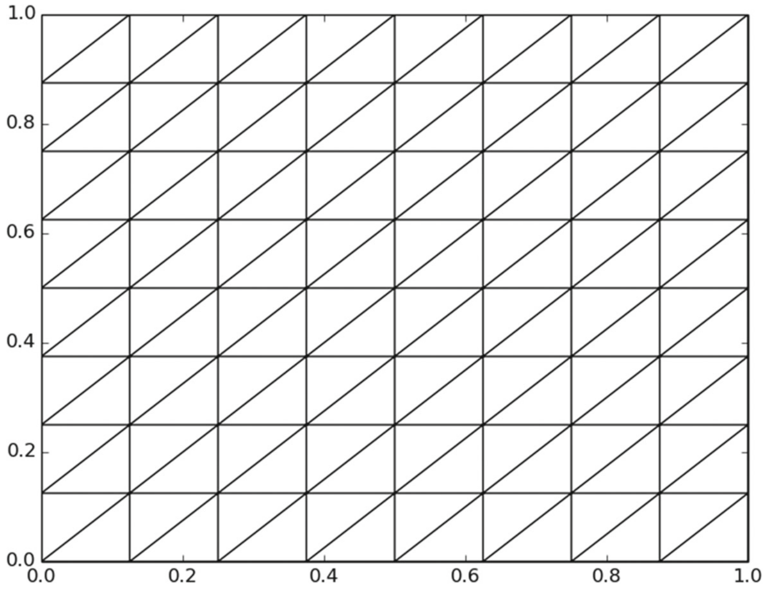

Fig. 1 A sample 8×8 mesh for our numerical test

errors $||\boldsymbol{E}_h^{n+1} - \boldsymbol{E}(t_{n+1})||$, $||\boldsymbol{E}_h^{n+1} - \boldsymbol{E}(t_{n+1})||$, and $||H_h^{n+\frac{1}{2}} - H(t_{n+\frac{1}{2}})||$ obtained at the last time step. Table 1 shows clearly the convergence rate of $O(h^p)$ in the L^2 norm for $\boldsymbol{E}$ and $\boldsymbol{D}$ proved in Theorem 4.2, though we do not have theoretical convergence for H. The corresponding CPU times (in seconds) are presented in Table 1 too.

Example 2. This example mimics Example 2 of our previous simulation [29] by the new leap-frog scheme (4.1)–(4.3). No equation is to be solved in the cloaked region. To show the invisibility cloaking phenomenon, we have to cover the cloaking region by a vaccum region where the standard Maxwell's equations in vacuum has to be solved. This can be done easily since (2.1)–(2.3) can be reduced to Maxwell's equations in vacuum by ignoring (2.2) and choosing $\mu = 1$ in (2.3). More specifically, in implementation of (4.1)–(4.3), we do not update (4.2) in the vaccum region, instead of just updating $\boldsymbol{E}_h^{n+1} = \epsilon_0^{-1}\boldsymbol{D}_h^{n+1}$.

In this example, the cloaking region parameters $H_1 = 0.1$ m, $H_2 = 0.4$ m, $d = 0.4$ m, the expanded physical domain $[-0.6, 0.6]\, m \times [0, 0.6]\, m$ covers the cloaking region and is partitioned by an unstructured triangular mesh with mesh size $h = 0.01$ m. We use a time step $\tau = 10^{-13}$ s, and the classical Berenger perfectly matched layer (PML) of thickness $15h$. An incident Gaussian wave

$$H_z(x, y, t) = \sin(2\pi f)\exp(-\frac{|\boldsymbol{x} - \boldsymbol{x}_c|^2}{L^2})$$

is imposed along a slanted line segment with endpoints $(-d, d/2)$ and $(-d/2, d)$, where $\boldsymbol{x} = (x, y)$ denotes arbitrary point on this line segment, $\boldsymbol{x}_c$ is the midpoint of this segment, and $L = 0.25\sqrt{2}d$. Snapshots of the numerical magnetic fields

Table 1 Example 1: The L^2 errors obtained with pth order Nédélec curl conforming edge element for both $\boldsymbol{E}$ and $\boldsymbol{D}$, and $(p-1)$th order L^2 basis function for H

				$p = 1$			
Meshes	$\boldsymbol{E}$ errors	Rates	$\boldsymbol{D}$ errors	Rates	H errors	Rates	CPU time (s)
4×4	7.206185E-01	-	4.380836E-01	-	7.843464E-02	-	1.37
8×8	3.175072E-01	1.1824	1.930210E-01	1.1824	3.822308E-02	1.0370	2.20
16×16	1.599098E-01	0.9895	9.721346E-02	0.9895	1.971290E-02	0.9553	5.25
32×32	8.010566E-02	0.9972	4.869838E-02	0.9972	9.923606E-03	0.9902	16.04
64×64	4.007202E-02	0.9993	2.436085E-02	0.9993	4.969948E-03	0.9976	59.57
128×128	2.003843E-02	0.9998	1.218189E-02	0.9998	2.486090E-03	0.9993	231.06
				$p = 2$			
Meshes	$\boldsymbol{E}$ errors	Rates	$\boldsymbol{D}$ errors	Rates	H errors	Rates	CPU time (s)
4×4	2.915181E-01	-	1.772222E-01	-	6.410242E-02	-	1.44
8×8	8.015973E-02	1.8626	4.873254E-02	1.8626	3.168191E-02	1.0167	2.56
16×16	2.068081E-02	1.9545	1.257292E-02	1.9545	9.146830E-03	1.7923	6.54
32×32	5.213000E-03	1.9881	3.168988E-03	1.9882	2.386382E-03	1.9384	21.99
64×64	1.313512E-03	1.9886	7.938809E-04	1.9970	6.189831E-04	1.9468	88.97
128×128	3.346313E-04	1.9727	1.985734E-04	1.9992	1.726740E-04	1.8418	437.15

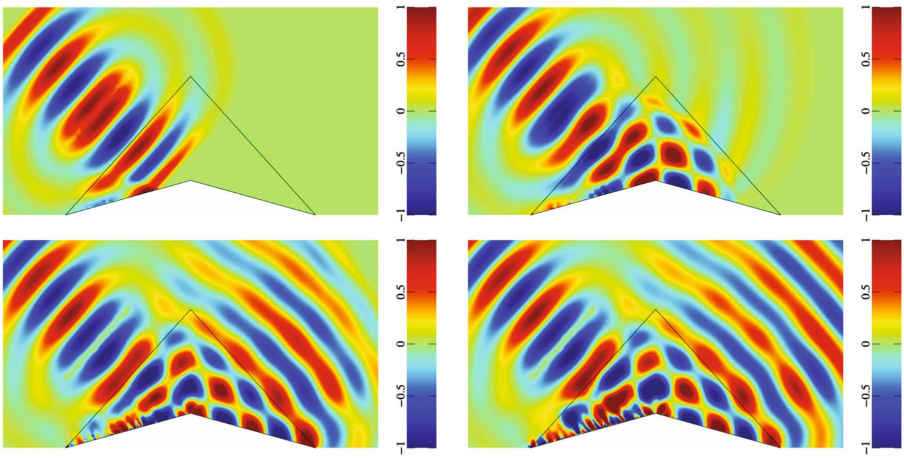

Fig. 2 Example 2 (with metamaterial). The magnetic fields H_z obtained at 12000, 24000, 40000, and 50000 time steps (oriented counterclockwise)

H_z obtained with frequency $f = 2$ GHz up to 50000 time steps are presented in Fig. 2, which clearly shows that the incident wave seems totally reflected from the flat ground. This reproduced the invisibility cloaking phenomenon obtained in [29] and also similar to the simulation obtained by COMSOL for the acoustic carpet cloak in [9, Fig. 7.7].

To appreciate the cloaking performance with metamaterial, we solve Example 2 again by replacing the cloaking region with air and keeping the rest parameters invariant. The obtained magnetic fields H_z at various time steps are presented in Fig. 3, which shows that the wave scatters. Hence, the cloak phenomenon disappears when the cloaking metamaterial is removed.

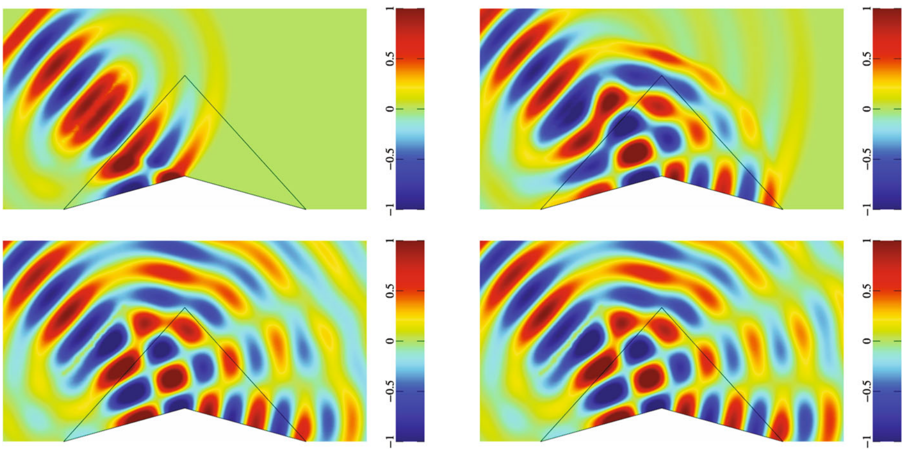

Fig. 3 Example 2 (without metamaterial). The magnetic fields H_z obtained at 12000, 24000, 40000, and 50000 time steps (oriented counterclockwise)

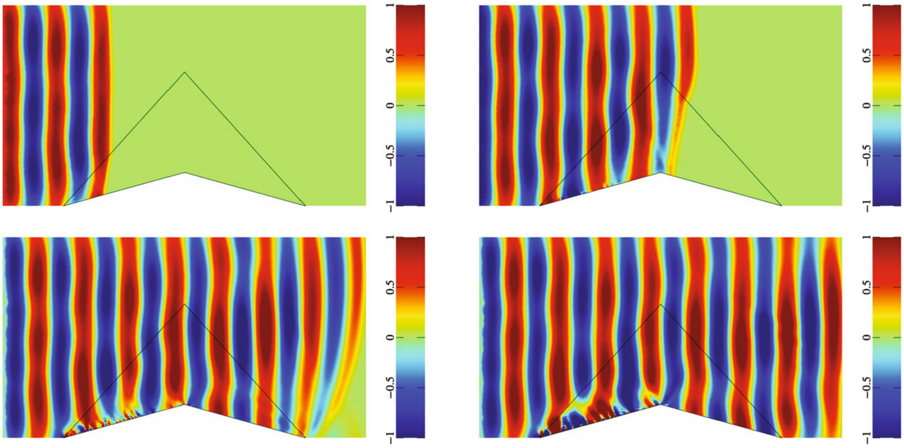

Fig. 4 Example 3. The magnetic fields H_z obtained at 12000, 24000, 40000, and 50000 time steps (oriented counterclockwise)

Example 3. This example mimics Example 1 of our previous simulation [29] by the new leap-frog scheme (4.1)–(4.3). Here we use the same physical parameters as Example 2, except that a plane incident source wave $H_z(x, y, t) = \sin(2\pi f)$ with frequency $f = 2$ GHz is imposed on edge $x = -0 : 6$ m. Snapshots of the obtained magnetic fields H_z are presented in Fig. 4, which shows that the wave resumes its plane wave patten after passing through the cloaked region. Hence, the invisibility cloaking phenomenon is achieved in this case.

6 Conclusions

In this paper, we proposed two new finite element schemes for solving the time-domain carpet cloak model. The major novelty of the paper is that both the Crank-Nicolson and leap-frog schemes are new, and they proved to be unconditionally stable and conditionally stable (under the usual CFL constraint $\tau = O(h)$), respectively. This overcomes the impractical CFL constraint $\tau = O(h^2)$ imposed on the stability analysis in previous works [29, 30]. Optimal error estimate is proved for the leap-frog scheme. An optimal error estimate can be similarly proved for the Crank-Nicolson scheme. We will continue exploring and analyzing more efficient algorithms such as LDG method [32, 45] for this interesting model in the future.

Acknowledgements J. Li would like to thank UNLV for granting his sabbatical leave during Spring 2021 so that he could have time working on this paper. We are grateful for two anonymous reviewers for their sightful comments on improving our paper.

Funding J. Li's work is supported by NSF grant DMS-2011943. C.-W. Shu's work is supported by NSF grant DMS-2010107 and AFOSR grant FA9550-20-1-0055. W. Yang's work is supported by Project of Scientifiic Research Fund of Hunan Provincial Science and Technology department (No. 2018WK4006), NSFC Projects 12171411 and 11771371.

Declarations

Conflict of interest The authors declare no competing interests.

References

1. Ammari, H., Kang, H., Lee, H., Lim, M., Yu, S.: Enhancement of near cloaking for the full Maxwell equations, SIAM. J. Appl. Math. **73**, 2055–2076 (2013)
2. Anees, A., Angermann, L.: Time domain finite element method for Maxwell's equations. IEEE Access **7**, 63852–63867 (2019)
3. Bao, G., Li, P., Wu, H.: An adaptive edge element method with perfectly matched absorbing layers for wave scattering by biperiodic structures. Math. Comput. **79**, 1–34 (2010)
4. Bokil, V.A., Cheng, Y., Jiang, Y., Li, F.: Energy stable discontinuous Galerkin methods for Maxwell's equations in nonlinear optical media. J. Comput. Phys. **350**, 420–452 (2017)
5. Brenner, S.C., Gedicke, J., Sung, L.-Y.: An adaptive p_1 finite element method for two-dimensional transverse magnetic time harmonic Maxwell's equations with general material properties and general boundary conditions. J. Sci. Comput. **68**(2), 848–863 (2016)
6. Brezzi, F., Douglas Jr., J., Marini, L.D.: Two families of mixed finite elements for second order elliptic problems. Numer. Math. **47**, 217–235 (1985)
7. Cassier, M., Joly, P., Kachanovska, M.: Mathematical models for dispersive electromagnetic waves: An overview. Comput. Math. Appl. **74**(11), 2792–2830 (2017)
8. Ciarlet Jr, P., Zou, J.: Fully discrete finite element approaches for time-dependent Maxwell's equations. Numer. Math. **82**, 193–219 (1999)
9. Li, J., Liang, Z., Zhu, J., Zhang, X.: Anisotropic metamaterials for transformation acoustics and imaging. In: Acoustic Metamaterials: Negative Refraction, Imaging, Sensing and Cloaking (eds. by R.V. Craster and S. Guenneau), Springer Series in Materials Science, Vol.166, pp.169-195 (2013)
10. Chung, E.T., Du, Q., Zou, J.: Convergence analysis of a finite volume method for Maxwell's equations in nonhomogeneous media, SIAM. J. Numer. Anal. **41**, 37–63 (2003)
11. Cockburn, B., Li, F., Shu, C.-W.: Locally divergence-free discontinuous Galerkin methods for the Maxwell equations. J. Comput. Phys. **194**, 588–610 (2004)
12. Demkowicz, L., Kurtz, J., Pardo, D., Paszynski, M., Rachowicz, W., Zdunek, A.: Computing with hp-adaptive finite elements. Vol. 2: Frontiers: Three Dimensional Elliptic and Maxwell Problems with Applications. CRC Press, Taylor and Francis (2008)
13. Duan, H., Liu, W., Ma, J., Tan, R.C.E., Zhang, S.: A family of optimal Lagrange elements for Maxwell's equations. J. Comput. Appl. Math. **358**, 241–265 (2019)
14. Greenleaf, A., Kurylev, Y., Lassas, M., Uhlmann, G.: Cloaking devices, electromagnetics wormholes and transformation optics. SIAM Rev. **51**, 3–33 (2009)
15. Guevara Vasquez, F., Milton, GW., Onofrei, D.: Broadband exterior cloaking. Opt. Express **17**, 14800–14805 (2009)
16. Hao, Y., Mittra, R.: FDTD Modeling of metamaterials: theory and applications artech house publishers (2008)
17. Hesthaven, J.S., Warburton, T.: Nodal discontinuous Galerkin methods: algorithms. Analysis, and Applications, Springer (2008)
18. Hiptmair, R.: Finite elements in computational electromagnetism. Acta Numerica **11**, 237–339 (2002)
19. Hong, J., Ji, L., Kong, L.: Energy-dissipation splitting finite-difference time-domain method for Maxwell equations with perfectly matched layers. J. Comput. Phys. **269**, 201–214 (2014)
20. Kohn, R.V., Onofrei, D., Vogelius, M.S., Weinstein, M.I.: Cloaking via change of variables for the Helmholtz equation. Comm. Pure Appl. Math. **63**, 973–1016 (2010)
21. Lassas, M., Salo, M., Tzou, L.: Inverse problems and invisibility cloaking for FEM models and resistor networks. Math. Mod. Meth. Appl. Sci. **25**(2), 309–342 (2015)
22. Lee, J.J.: A mixed method for time-transient acoustic wave propagation in metamaterials. J. Sci. Comput. **84**, 20 (2020)
23. Leonhardt, U.: Optical conformal mapping. Science **312**, 1777–1780 (2006)
24. Leonhardt, U., Tyc, T.: Broadband invisibility by non-Euclidean cloaking. Science **323**, 110–112 (2009)

25. Li, J.: Two new finite element schemes and their analysis for modeling of wave propagation in graphene. Results in Applied Mathematics 9 **100136**, 21 (2021)
26. Li, J., Hesthaven, J.S.: Analysis and application of the nodal discontinuous Galerkin method for wave propagation in metamaterials. J. Comput. Phys. **258**, 915–930 (2014)
27. Li, J., Huang, Y.: Time-domain finite element methods for Maxwell's equations in metamaterials, Springer Series in Computational Mathematics, vol.43 Springer (2013)
28. Li, J., Huang, Y., Yang, W.: Well-posedness study and finite element simulation of time-domain cylindrical and elliptical cloaks. Math. Comp. **84**, 543–562 (2015)
29. Li, J., Huang, Y., Yang, W., Wood, A.: Mathematical analysis and time-domain finite element simulation of carpet cloak, SIAM. J. Appl. Math. **74**(4), 1136–1151 (2014)
30. Li, J., Meng, C., Huang, Y.: Improved analysis and simulation of a time-domain carpet cloak model, Comput. Methods Appl. Math. **19**(2), 359–378 (2019)
31. Li, J., Pendry, J.B.: Hiding under the carpet: a new strategy for cloaking. Phys. Rev. Lett. **101**, 203901 4 (2008)
32. Li, J., Shi, C., Shu, C.-W.: Optimal non-dissipative discontinuous Galerkin methods for Maxwell's equations in Drude metamaterials. Comput. Math. Appl. **73**, 1760–1780 (2017)
33. Li, W., Liang, D., Lin, Y.: A new energy-conserved s-fdtd scheme for maxwell's equations in metamaterials. Int. J. Numer. Anal. Mod. **10**, 775–794 (2013)
34. Liu, R., Ji, C., Mock, J.J., Chin, J.Y., Cui, T.J., Smith, D.R.: Broadband ground-plane cloak. Science **323**, 366–369 (2009)
35. Logg, A., Mardal, K.-A., Wells, G.N. (eds.): Automated solution of differential equations by the finite element method: the FEniCS book. Springer, Berlin (2012)
36. Monk, P.: Analysis of a finite element method for Maxwell's equations, SIAM. J. Numer. Anal. **29**, 714–729 (1992)
37. Monk, P.: Finite element methods for maxwell's equations oxford university press (2003)
38. Nédélec, J.-C.: Mixed finite elements in $\mathcal{R}^3$. Numer. Math. **35**(3), 315–341 (1980)
39. Nédélec, J.-C.: A new family of mixed finite elements in $\mathcal{R}^3$. Numer. Math. **50**(1), 57–81 (1986)
40. Nicaise, S., Venel, J.: A posteriori error estimates for a finite element approximation of transmission problems with sign changing coefficients. J. Comput. Appl. Math. **235**, 4272–4282 (2011)
41. Pendry, J.B., Schurig, D., Smith, D.R.: Controlling electromagnetic fields. Science **312**, 1780–1782 (2006)
42. Quarteroni, A., Valli, A.: Numerical approximation of partial differential equations, Springer Ser. Comput Math, vol. 23. Springer, Berlin (1994)
43. Raviart, P.A., Thomas, J.M.: A mixed finite element method for 2nd order elliptic problems. In: Mathematical aspects of the finite element method (eds. by I. Galligani and E. Magenes). Lecture Notes in Mathematics, Vol. 606. Berlin-Heidelberg-New York: Springer, pp. 292-315 (1977)
44. Scheid, C., Lanteri, S.: Convergence of a discontinuous Galerkin scheme for the mixed time domain Maxwell's equations in dispersive media, IMA. J. Numer. Anal. **33**(2), 432–459 (2013)
45. Shi, C., Li, J., Shu, C.-W.: Discontinuous Galerkin methods for Maxwell's equations in Drude metamaterials on unstructured meshes. J. Comput. Appl. Math. **342**, 147–163 (2018)
46. Werner, D.H., Kwon, D.-H. (eds.): Transformation electromagnetics and metamaterials: fundamental principles and applications. Springer, Berlin (2013)
47. Xie, Z., Wang, J., Wang, B., Chen, C.: Solving Maxwell's equation in meta-materials by a CG-DG method. Commun. Comput. Phys. **19**(5), 1242–1264 (2016)
48. Yang, Z., Wang, L.L.: Accurate simulation of ideal circular and elliptic cylindrical invisibility cloaks. Commun. Comput. Phys. **17**(3), 822–849 (2015)
49. Yang, Z., Wang, L.-L., Rong, Z., Wang, B., Zhang, B.: Seamless integration of global Dirichlet-to-Neumann boundary condition and spectral elements for transformation electromagnetics. Comput. Methods Appl. Mech. Engrg. **301**, 137–163 (2016)